PACIFIC ISLANDS FISHERIES SCIENCE CENTER

An Investigation of Alternative Production Models to Assess the Hawaiian Bottomfish Complex

By

Jon Brodziak

July 2007

Administrative Report H-07-01

About this report

Pacific Islands Fisheries Science Center Administrative Reports are issued to promptly disseminate scientific and technical information to marine resource managers, scientists, and the general public. Their contents cover a range of topics, including biological and economic research, stock assessment, trends in fisheries, and other subjects. Administrative Reports typically have not been reviewed outside the Center. As such, they are considered informal publications. The material presented in Administrative Reports may later be published in the formal scientific literature after more rigorous verification, editing, and peer review.

Other publications are free to cite Administrative Reports as they wish provided the informal nature of the contents is clearly indicated and proper credit is given to the author(s).

Administrative Reports may be cited as follows:

> *Author. Date. Title*. Pacific Islands Fish. Sci. Cent., Natl. Mar. Fish. Serv., NOAA, Honolulu, HI 96822-2396. Pacific Islands Fish. Sci. Cent. Admin. Rep. H-*XX-YY*, *xx* p.

For further information direct inquiries to

Chief, Scientific Information Services
Pacific Islands Fisheries Science Center
National Marine Fisheries Service
National Oceanic and Atmospheric Administration
U.S. Department of Commerce
2570 Dole Street
Honolulu, Hawaii 96822-2396

Phone: 808-983-5386
Fax: 808-983-2902

Pacific Islands Fisheries Science Center
Administrative Report H-07-01

An Investigation of Alternative Production Models to Assess the Hawaiian Bottomfish Complex

By

Jon Brodziak

Pacific Islands Fisheries Science Center
National Marine Fisheries Service
2570 Dole Street
Honolulu, Hawaii 96822-2396
E-mail: Jon.Brodziak@noaa.gov

July 2007

ABSTRACT

The status of the bottomfish complex of the Hawaiian Islands is currently assessed using a Schaefer surplus production model. Estimation of model parameters is based on fitting time series of catch-per-unit-effort (CPUE) data using an ad hoc, nonlinear least-squares approach. This paper investigates the application of a more formal Bayesian statistical framework to estimate parameters of alternative bottomfish surplus production models. The Bayesian approach provides direct estimates of parameter uncertainty that are easy to interpret and are appropriate for risk analysis. The models include both process error for biomass production dynamics and observation error for the CPUE data. Alternative models are formulated and contrasted using Akaike's information criterion. Model averaging is applied to meld results of competing models where appropriate. The issue of whether model parameters such as intrinsic growth rate, carrying capacity, and catchability, are reliably estimable is also addressed. The modeling focuses on estimating the hypothetical status of the bottomfish complex of the main Hawaiian Islands and also includes linked estimation procedures to assess the status of bottomfish in the Mau and Ho'omalu Zones as well as the Hawaiian Archipelago using alternative production models. The sensitivity of modeling results to prior distributions and model assumptions is evaluated. Potential improvements to the data collection and modeling approach used to assess the status of the Hawaiian bottomfish complex are discussed.

CONTENTS

Page

INTRODUCTION

The Hawaiian Islands bottomfish complex is made up of a set of snappers, groupers, and jacks that inhabit depths of up to 100 fathoms off the Hawaiian Archipelago. Although the deepwater bottomfish complex in Hawaii has been commercially fished since at least the early-1900s (Haight et al., 1993), initial assessments of Hawaiian bottomfish began in the 1980s. Bottomfish assessments have typically used a multispecies production modeling approach. The geographic range of bottomfishes has been divided into three major zones for assessment purposes. These fishing zones are the main Hawaiian Islands (MHI), the Mau Zone and the Ho'omalu Zone (Fig. 1).

In the current assessment of the Hawaiian bottomfish complex, the dynamics of the multispecies complex in each zone is assessed using a Schaefer surplus production model (Moffitt et al., 2006). Commercial catches and catch rates have been collected from the MHI since 1948 and from the Mau and Ho'omalu Zones since 1988. The differences in catch time series limit the surplus production modeling to 1988-2004 in the Mau and Ho'omalu Zones while the surplus production model for the MHI extends from 1948 to 2004. The current assessment assumes that the intrinsic growth rate of Hawaiian bottomfish is similar across zones. Thus, a single intrinsic growth rate is estimated for all zones in the surplus production models. The current assessment also assumes that the relative amount of bottomfish habitat in each zone is proportional to the linear extent of its 100-fathom contour. The carrying capacity of the MHI is directly estimated while the carrying capacities of the Mau and Ho'omalu Zones are set based on the ratio of MHI habitat to Mau or Ho'omalu habitat multiplied by the carrying capacity estimate for the MHI. Thus, a single carrying capacity parameter is determined for the MHI and the carrying capacities of the Mau and Ho'omalu Zones are set to be proportional to the amount of their bottomfish habitat relative to the MHI. Overall, the bottomfish surplus production model for the current assessment includes linkages between the intrinsic growth rates and carrying capacities estimated for each fishing zone.

Status determination of the Hawaiian Islands bottomfish complex is based on the habitat-weighted average of the model results by fishing zone. That is, the status of the complex is assessed for the entire Hawaiian Archipelago as specified in the Fishery Management Plan. This status determination is based on the assumption that there is sufficient interchange among adult and larval fishes of the three zones to treat them as a single management unit.

The data available for assessing Hawaiian Islands bottomfish status are limited primarily to fishery-dependent data in the current assessment model. There are currently no fishery-independent measures of relative or absolute bottomfish abundance. Trends in relative abundance are based solely on fishery catch-per-unit-effort (CPUE) data. To address the fact that fishing practices have changed over time, the current assessment assumes that the fishery catchability coefficient has increased over time. In particular, the current assessment assumes four separate time periods in which catchability remains constant through each period. The relative catchabilities of the four periods were set based on limited field observations, anecdotal knowledge, and subjective judgment. Under this approach, the fishery catchability

coefficient for one time period was estimated in the surplus production modeling, and the others were set based on their assumed relative catchabilities.

The estimation procedure used in the current assessment is nonlinear least squares. There are no explicit assumptions regarding the error structure for the parameter fitting procedure, however. As a result, no estimates of parameter uncertainty are available in the current assessment model. Although this approach is straightforward, it includes ad hoc elements and does not provide variance estimates for model parameters or other outputs. The lack of variance estimates makes it difficult to weigh the risks associated with alternative management actions.

This paper investigates the application of a more formal Bayesian statistical framework to estimate parameters of alternative bottomfish surplus production models. The Bayesian approach provides direct estimates of parameter uncertainty that are easy to interpret and are appropriate for risk analysis. The models include both process error for biomass production dynamics and observation error for the CPUE data. Alternative models are formulated and contrasted using Akaike's information. Model averaging is applied to meld results of competing models where appropriate. The issue of whether model parameters such as intrinsic growth rate, carrying capacity, and catchability are reliably estimable is also addressed. The modeling focuses on estimating the hypothetical status of the bottomfish complex of the main Hawaiian Islands and also includes linked estimation procedures to assess the status of bottomfish in the Mau and Ho'omalu Zones as well as the Hawaiian Archipelago using alternative production models. The sensitivity of modeling results to prior distributions and model assumptions is evaluated. Potential improvements to the data collection and modeling approach used to assess the status of the Hawaiian bottomfish complex are discussed.

METHODS

Fishery Data

The fishery-dependent catch data for assessing the Hawaiian bottomfish complex were taken from the most recent assessment (Moffitt et al., 2006). Commercial catch data for the primary bottomfish species (Table 1) were available for MHI and the Northwestern Hawaiian Islands (NWHI) (Mau and Ho'omalu Zones) during 1948-2004. Commercial bottomfish catch in the MHI peaked in the late 1980s and has declined since then (Fig. 2). Catches in the Mau and Ho'omalu Zones have fluctuated without trend since the mid 1980s (Fig. 2).

Estimates of commercial fishery CPUE were also collected from Moffitt et al. (2006) for the MHI during 1948–2004 and for NWHI during 1988–2004 (Fig. 3). The CPUE time series for MHI exhibits a long-term decline (Fig. 4A) with an increase in fishing effort since the early 1980s. In the Mau Zone, CPUE has fluctuated without trend at low fishing effort during 1988-2004 (Fig. 4B). In the Ho'omalu Zone, CPUE has declined since 1988, while fishing effort has remained relatively stable since the early 1990s (Fig. 4C). Overall, the MHI and Ho'omalu Zones both exhibit declining CPUE over the past decade.

Production Model

The alternative bottomfish production models are formulated as Bayesian-state space models with explicit process and observation error terms (see, for example, Meyer and Millar, 1999). In this case, the unobserved biomass states are estimated from the observed relative abundance indices (CPUE) and catches based on an observation error likelihood function and prior distributions for model parameters (θ). The observation error likelihood measures the discrepancy between observed and model predictions of CPUE.

The process dynamics are based on a power function surplus production model with an annual time step. Under this 3-parameter model, current biomass (B_T) depends on the previous biomass, catch (C_{T-1}), the intrinsic growth rate (R), carrying capacity (K), and a production shape parameter (M) for $T = 2,\ldots, N$.

(1) $$B_T = B_{T-1} + R \cdot B_{T-1}\left(1 - \left(\frac{B_{T-1}}{K}\right)^M\right) - C_{T-1}$$

The shape parameter $M > 0$ determines where surplus production peaks as biomass varies in proportion to carrying capacity (Fig. 5). If $0 < M < 1$, surplus production peaks when biomass is below ½ of K. If $M > 1$, then surplus production is highest when biomass is above ½ of K. If $M = 1$, the production model is identical to the Schaefer model where maximum surplus production occurs when biomass is equal to ½ of K. The values of biomass and harvest rate that maximize surplus production are relevant for fishery management under the Magnuson Fishery Conservation and Management Act as reauthorized in 1996. For the discrete-time power function model, the biomass that maximizes surplus production (B_{MSY}) is

(2) $$B_{MSY} = K \cdot \left(M + 1\right)^{\frac{-1}{M}}$$

The corresponding harvest rate that maximizes surplus production (H_{MSY}) is

(3) $$H_{MSY} = R\left(1 - \frac{1}{M+1}\right)$$

and the maximum surplus production (MSY) is

(4) $$MSY = R\left(1 - \frac{1}{M+1}\right) \cdot K\left(M+1\right)^{\frac{-1}{M}}$$

The power function model can be reparameterized in terms of the proportion of carrying capacity ($P = B/K$) to improve the efficiency of the Markov Chain Monte Carlo estimation algorithm. Based on this parameterization, the process dynamics for the power function model are

(5) $$P_T = P_{T-1} + R \cdot P_{T-1}\left(1 - P_{T-1}^M\right) - \frac{C_{T-1}}{K}$$

The process dynamics are subject to natural variation as a result of fluctuations in life history parameters, trophic interactions, environmental conditions and other factors. In this context, the process error can be thought of as the joint effect of a large number of random multiplicative events which combine to form a multiplicative lognormal process under the Central Limit Theorem. Given this, the process error terms are independent and lognormally distributed random variables $\eta_T = e^{U_T}$ where the U_T are normal random variables with mean 0 and variance σ^2.

The state equations define the stochastic process dynamics by relating the unobserved biomass states to the observed catches and the population dynamics parameters. Given the lognormal process error assumption, the state equations for the initial time period $T = 1$ and subsequent periods $T > 1$ are

(6)
$$P_1 = \eta_1$$
$$P_T = \left(P_{T-1} + R \cdot P_{T-1}\left(1 - P_{T-1}^M\right) - \frac{C_{T-1}}{K} \right) \cdot \eta_T$$

These equations set the prior distribution for the proportion of carrying capacity, $p(P_T)$, in each time period T, conditioned on the previous proportion.

Observation Error Model

The observation error model relates the observed fishery CPUE to the biomass of the bottomfish complex. Here it will be assumed that the CPUE index (I) is proportional to biomass with catchability coefficient Q

(7) $$I_T = QB_T = QKP_T$$

The assumption that Q is constant through time or CPUE is strictly proportional to biomass is relaxed in some of the alternative models below.

The observed CPUE dynamics are also subject to natural sampling variation and will be assumed to be lognormally distributed. The observation errors are $\nu_T = e^{V_T}$ where the V_T are iid normal random variables with zero mean and variance τ^2. Given this, the observation equations for $T = 1,\ldots, N$ are

(8) $$I_T = QKP_T \cdot \nu_T$$

This specifies the observation error likelihood function $p(I_T|\theta)$ for each period.

Prior Distributions

Under the Bayesian paradigm, prior distributions are employed to quantify existing knowledge (or the lack thereof) of the likely value of model parameters and the unobserved biomass states. In this context, the model parameters consist of the carrying capacity, intrinsic growth rate, shape parameter, catchability, the process and observation error variances, and the initial biomass as a proportion of carrying capacity. Unobserved biomass states are the proportions of carrying capacity, P_T, for $T > 1$, conditioned on the previous proportion. In general, prior information was used where it was available.

Prior for Carrying Capacity

The prior distribution for the carrying capacity $p(K)$ of MHI was chosen to be a diffuse normal distribution with mean $\left(\mu_K\right)$ and variance $\left(\sigma_K^2\right)$ parameters

$$\textbf{(9)} \qquad p(K) = \frac{1}{\sqrt{2\pi}\sigma_K}\exp\left(-\frac{\left(K-\mu_K\right)^2}{2\sigma_K^2}\right)$$

The mean parameter was set to be 2 million pounds based on the numerical results in Moffitt et al. (2006).The variance parameter was set to 100 million pounds to allow for a wide range of carrying capacity values. In effect, this was a relatively uninformative prior for K. The values of carrying capacity for the Mau and Ho'omalu Zones were set based on the estimate of K and the relative habitat weights for the three bottomfish management zones ($W_{\text{MHI}} = 0.447$, $W_{\text{Mau}} = 0.124$, $W_{\text{Ho'omalu}} = 0.429$) as in the current assessment (Moffitt et al., 2006). Thus, the carrying capacities of the Mau and Ho'omalu Zones were $0.277K$ and $0.960K$, respectively.

Prior for Intrinsic Growth Rate

The prior distribution for intrinsic growth rate $p(R)$ was chosen to be an offset beta distribution with parameters c and d and offset Δ:

$$\textbf{(10)} \qquad p(R) = \Delta + \left(1-\Delta\right)\frac{\Gamma\left(c+d\right)}{\Gamma\left(c\right)\Gamma\left(d\right)}\cdot x^{c-1}\left(1-x\right)^{d-1}$$

This choice constrained the intrinsic growth rate estimate to be within the interval $\left[\Delta, 1\right]$. In this context, Δ and 1 were upper and lower bounds on the intrinsic growth rates. The offset Δ was set to be 0.1 based on the estimate from Moffitt et al. (2006) of $R = 0.46$ which indicated that values lower than 0.1 or greater than 1 were unlikely. This range was consistent with the fact that the bottomfish complex included snappers with relatively high values of natural mortality ($M > 0.25$) and moderate values of Brody growth coefficients (Martinez-Andrade,

2003). The central tendency of the intrinsic growth rate prior was approximated using the mean generation time of a hypothetical bottomfish species with egg survival of $^1/_{10000}$, natural mortality of 0.3, full maturation at age 3 producing 100,000 eggs, and an 8% annual increase in fecundity from age 4 to age 15. This life history pattern was considered to be plausible for opakapaka, one of the more abundant species in the bottomfish complex. Assume these life history parameters lead to an intrinsic growth rate of $R \approx 0.57$ by using the mean generation time approximation of intrinsic growth rate (McAllister et al., 2001). Although this is a crude approximation for R, it gives a rough idea of the scale of the prior. The values of c and d were set to 12.0. This implied that the mean of the beta distribution was 0.5 with a coefficient of variation (CV) of 20%. Given this, the mean of the offset beta distribution was then $\mu_R = 0.55$ with a CV of 18%. Overall, the mean of this informative prior for R was about 25% higher than the value reported in Moffitt et al. (2006). Sensitivity to the choice of the informative prior distribution for R is examined below.

Prior for Production Shape Parameter

The prior distribution for the production function shape parameter $p(M)$ was chosen to be a gamma distribution with scale parameter λ and shape parameter k:

$$\textbf{(11)} \qquad p(M) = \frac{\lambda^k M^{k-1} \exp(-\lambda M)}{\Gamma(k)}$$

The values of the scale and shape parameters were set to $\lambda = k = 2$. This choice implied that the mean of $p(M)$ was $\mu_M = 1$, which corresponds to the value of M under the Schaefer production model. This choice also implied that the CV of the shape parameter prior was 71%. In effect, the shape parameter prior was centered on a Schaefer model as the default with substantial flexibility to estimate a nonsymmetric production function.

Prior for Catchability

The prior for catchability $p(Q)$ was chosen to be a diffuse inverse-gamma distribution with scale parameter λ and shape parameter k.

$$\textbf{(12)} \qquad p(Q) = \frac{\lambda^k Q^{-(k+1)}}{\Gamma(k)} \exp\left(\frac{-\lambda}{Q}\right)$$

The scale and shape parameters were set to be $\lambda = k = 0.001$. This choice of parameters implies that $1/Q$ has a mean of 1 and a variance of 1000. As a result, the prior for catchability is effectively $p(Q) \propto Q^{-1}$. Since $1/Q$ is unbounded at $Q = 0$, an additional numerical constraint that Q lie within the interval [0.0001, 10] was imposed.

Priors for Error Variances

Priors for the process error variance $p(\sigma^2)$ and observation error variance $p(\tau^2)$ were chosen to be inverse-gamma distributions, a natural choice for dispersion priors (Congdon, 2001). For the process error variance prior, the scale parameter was set to $\lambda = 4$ and the shape parameter was $k = 0.01$. This choice of parameters produces an 80% confidence interval of approximately [0.04, 0.08] for σ. Similarly, for the observation error variance prior, the scale parameter was set to $\lambda = 2$ and the shape parameter was $k = 0.01$. This choice of parameters gives an 80% confidence interval of approximately [0.05, 0.14] for τ. Thus, the observation error variance was assumed to be greater than the process error variance.

Priors for Proportions of Carrying Capacity

Prior distributions for the time series of biomass in proportion to carrying capacity, $p(P_T)$, are determined by the lognormal distributions specified in the process dynamics. The mean proportion of carrying capacity for the initial time period was set to be unity for each region in the absence of information on the likely value. Based on previous applications of this type of Bayesian surplus production model, the relative trends in biomass and fishing mortality estimates were not expected to be influenced by the choice of the mean of the lognormal distribution. This expectation was evaluated in the sensitivity analyses below.

Posterior Distribution

The posterior distribution needs to be calculated to make inferences about the model parameters. From Bayes' theorem, the posterior distribution given catch and CPUE data D, $p(\theta|D)$, is proportional to the product of the priors and the likelihood of the CPUE data.

$$\textbf{(13)} \qquad p(\theta \mid D) \propto p(K)\,p(R)\,p(M)\,p(Q)\,p(\sigma^2)\,p(\tau^2)\prod_{T=1}^{N} p(P_T)\prod_{T=1}^{N} p(I_T \mid \theta)$$

There is no closed form expression to determine parameter estimates from the posterior distribution in (13).

Under the Bayesian paradigm, parameter estimation for multiparameter nonlinear models, such as the bottomfish production model, is typically based on simulating a large number of independent samples from the posterior distribution. In this case, Markov Chain Monte Carlo (MCMC) simulation (Gilks et al., 1996) was applied to numerically generate a sequence of samples from the posterior distribution. I used the WINBUGS software (Spiegelhalter et al., 2003) to set the initial conditions, perform the MCMC calculations, and summarize the results (see Appendix).

MCMC simulations were conducted in an identical manner for each of the alternative models described below. Two chains of 210,000 samples were simulated in each model run. The first 10,000 samples of each chain were excluded from the estimation process. This burn-

in period removed any dependence of the MCMC samples on the initial conditions. Next, each chain was thinned by 2 to remove autocorrelation. That is, every other sample was used for inference. As a result, 100,000 samples from the posterior were used for summarizing model results. Convergence of the MCMC simulations to the posterior distribution was checked using the Brooks-Gelman-Rubin (BGR) convergence diagnostic (Brooks and Gelman, 1998). This diagnostic was monitored for several key model parameters (intrinsic growth rate, carrying capacity, production function shape parameter, catchability, initial proportion of carrying capacity) as well as the root-mean squared error (RMSE).

Goodness-of-Fit Criteria

Model residuals were used to measure the goodness of fit of the alternative production models. Residuals for the CPUE series are the log-scale observation errors ε_T.

(14) $$\varepsilon_T = \ln\left(I_T\right) - \ln\left(QKP_T\right)$$

Non-random patterns in the residuals indicate that the observed CPUE does not conform to one or more model assumptions. The RMSE of the CPUE fit provided another diagnostic of the model goodness of fit with lower RMSE indicating a better fit when comparing models with the same number of parameters. The Akaike Information Criterion (AIC) can be used to contrast non-nested models with different numbers of parameters (p) applied to the same data (Burnham and Anderson, 2002), where

(14) $$AIC = N \cdot \ln\left(\frac{\sum_{T=1}^{N} \varepsilon_T^2}{N}\right) + 2p$$

The first term in the expression for AIC is equivalent to minus 2 times the log-likelihood, a measure of goodness of fit, while the second term is a parameter penalty. In this application, a bias-corrected version of AIC (AICC) was used for model comparison since the ratio of the sample size to the number of free parameters is less than 10 (see, for example, Burnham and Anderson, 2002).

(15) $$AICC = AIC + \frac{2p\left(p+1\right)}{N-p-1}$$

The model with the lowest value of information criterion among competing models gives the best fit to the data. To rank a set of models, it is convenient to use the difference (Δ_k) in AIC value (AIC_k) from the best fitting model (AIC_{MIN}) where, for model k, $\Delta_k = AIC_k - AIC_{MIN}$. The AIC differences determine the relative likelihood of alternative models. The likelihood of model k (L_k), for example, is proportional to the exponential of the AIC difference

(16) $$L_k \propto \exp\left(-\frac{1}{2}\Delta_k\right)$$

The relative weight of evidence in favor of each model, also known as the Akaike weight (w_k), can be obtained by normalizing the model likelihood across the set of operating models

(16) $$w_k = \frac{\exp\left(-\frac{1}{2}\Delta_k\right)}{\sum_j \exp\left(-\frac{1}{2}\Delta_j\right)}$$

The Akaike weights sum to one and provide a measure of the probability that each model is true given the fixed data. In practice, the ratios of the Akaike weights will be used to characterize the evidence in favor or against a given model and to average results from competing models.

Interpreting the Akaike weights as posterior model probabilities, the model-averaged value of a parameter θ conditioned on the observed data *D* is the weighted sum of the expected values of θ under the alternative models M_k

(17) $$E(\theta \mid D) = \sum_k w_k E(\theta \mid M_k, D)$$

Similarly, the variance of the parameter θ is equal to the weighted sum of the variances of θ under the alternative models as adjusted by their conditional means

(18) $$Var(\theta \mid D) = \sum_k w_k \left(Var(\theta \mid M_k, D) + E(\theta \mid M_k, D)^2\right) - E(\theta \mid D)^2$$

This estimate of the variance of θ accounts for both parametric and model uncertainty.

Alternative Models

Two sets of alternative production models were investigated: single zone and multizone. A set of four models were developed for a single zone, MHI. This was conducted to evaluate the status of the MHI in isolation and for comparison with the MHI estimates in Moffitt et al. (2006). A second set of 10 models were developed for the MHI, the Mau Zone, and the Ho'omalu Zone all together. In these models, parameter estimates of carrying capacity or intrinsic growth or production function shape were linked across zones, similar to the analysis in Moffitt et al. (2006). This was conducted to discern whether there was sufficient data to assess status in the separate zones as well as for comparison with the results of Moffitt et al. (2006).

Main Hawaiian Islands Models

Each of the four alternative models for the MHI was fit using the MHI catch and CPUE data for 1948–2004 (Table 2.1). *Model 1 incorporated power function dynamics and a constant fishery catchability.* This baseline model allowed for nonsymmetric production from the bottomfish complex. It also used a simpler constant fishery catchability assumption than the 4-period fishery catchability assumption in Moffitt et al. (2006).

The second MHI model was identical to the first but included catch errors (Table 2.1). This was conducted to investigate the effects of underreported commercial catch on parameter estimates. Annual catch error distributions were assumed for two time periods: 1948–1989 and 1990–2004. Annual catch errors were assumed to be uniformly distributed between 0% to 20% for the 1948–1989 period. This assumption was modeled by including a uniform prior on annual catch. For the 1990–2004 period, catch errors were believed to be relatively low (Bob Moffitt, pers. comm.) and the annual catch error was assumed to be uniformly distributed between 0% and 2%.

The third MHI model was identical to the first (Table 2.1) but incorporated the four period catchability assumption from Moffitt et al. (2006). The four time periods for Q were chosen to reflect changes in the fishery. In this approach, changes in Q were assessed relative to the estimate for 1985–1991 (Q_{BASELINE}). Q was assumed to be 70% of Q_{BASELINE} during 1948–1967. – was assumed to increase to 80% of Q_{BASELINE} during 1968–1984. In the current period (1992–2004), Q was assumed to be 120% of Q_{BASELINE}.

The fourth MHI model incorporated similar assumptions as in model 1 but used a Schaefer curve instead of the power function (Table 2.1). This model explored whether assuming Schaefer dynamics provided a more parsimonious fit to the MHI data.

Archipelago Models

The 10 alternative multizone models for the Hawaiian Archipelago were simultaneously fit to the MHI CPUE data for 1948–2004 and the Mau and Ho'omalu CPUE data for 1988–2004 (Table 2.2). These multizone models provided a closer approximation to the current assessment model than the single-zone models since they fit CPUE data in each fishing zone.

Model 5 was an extension of model 4 to incorporate the Mau and Ho'omalu Zone data. In this case, the carrying capacities of the Mau and Ho'omalu Zones were assumed to be proportional to their relative habitat. The intrinsic growth rate was assumed to be the same across zones, and each zone was assumed to have a constant catchability through time.

Model 6 was the same as model 5 but incorporated the 4-period catchability assumption from Moffitt et al. (2006). This was conducted to evaluate whether constant or time-varying catchability provided a better fit for a multizone model. In effect, model 6 was

the baseline multizone model since it most closely reflected the modeling assumptions in Moffitt et al. (2006).

Model 7 was identical to model 5 with the exception that it used power function dynamics with identical shape parameters across zones (Table 2.2). This was conducted to evaluate whether a shape parameter would improve the fit to the multizone data.

Model 8 was a variant of model 6 that estimated a separate intrinsic growth rate for each zone (Table 2.2). This was conducted to evaluate whether productivity differed among zones assuming time-varying catchability for the MHI.

Model 9 was an extension of model 8 that included a density-dependent catchability model for the MHI (Table 2.2). In this case, the observation equation for the MHI CPUE was modified to include an exponent (q_{EXP}) which had a uniform prior distribution on the interval [0.1, 10]

(17) $$I_T = Q\left(KP_T\right)^{q_{EXP}} \cdot \nu_T$$

Thus, model 9 had one more free parameter to be estimated than model 8.

Model 10 was identical to model 8 but estimated carrying capacity capacities for each zone rather than assuming that zonal differences in K were proportional to their relative bottomfish habitat (Table 2.2). This was conducted to investigate whether there was sufficient information to freely estimate carrying capacities for each fishing zone.

Model 11 was a variant of model 7 that estimated intrinsic growth rates for each zone (Table 2.2). This was conducted to investigate whether a common shape parameter and separate intrinsic growth rates were estimable by fishing zone.

Model 12 was identical to model 11 but assumed power function dynamics for the MHI and Schaefer dynamics for the Mau and Ho'omalu Zones (Table 2.2). This was conducted to see if there was sufficient information to estimate a shape parameter for the zone with the longest time series.

Model 13 was a variant of model 8 that used three periods for time-varying Q instead of the four periods from Moffitt et al. (2006). In this case, the 1st and 2nd periods were combined into a single period (1948–1984) in which Q was set to be 80% of $Q_{BASELINE}$. This was conducted to see if there was any improvement in model fit with a simpler assumption about the temporal changes in Q.

Model 14 was a variant of the baseline model 6 that included a simple estimate of recreational bottomfish catch (Table 2.2). In this case, it was assumed that recreational bottomfish catch was 30% of the commercial catch through time. This assumption was based on a short-term recreational angler survey conducted in 1990–1991 (Hamm and Lum, 1992). In particular, Hamm and Lum (1992, Table 5) estimated the recreational bottomfish catch on Oahu during March1990 to February 1991 to be 178,969 pounds, roughly 30% of the

commercial bottomfish catch (590,450 lbs) from MHI during calendar year 1990. Overall, model 14 was used to evaluate the potential effect of including recreational catch on reference points and status determination criteria.

Environmental Forcing

An exploratory investigation of the association between the best-fitting multizone model residuals and sea surface height (SSH) anomalies was also conducted. This was done to evaluate whether additional variation in observed CPUE values for each zone could be explained by zonal SSH indices from satellite altimeter data, a proxy for local ocean productivity. SSH anomalies from the merged satellite altimeter data set were obtained from AVISO (e.g., Ducet et al., 2000) during 1993–2000. Annual SSH anomaly data were averaged over winter months (January–March) for representative rectangular regions within each zone. The southwest and northeast corners of the rectangular regions were: MHI (18˚N 160˚W and 20˚N 154˚W), Mau Zone (22˚N 164˚W and 24˚N 162˚W), and Ho'omalu Zone (27˚N 179˚W and 29˚N 176˚W). Pearson correlations were used to measure the association between the zonal CPUE residuals and the contemporaneous SSH anomaly series.

Sensitivity Analyses

Two sensitivity analyses were also conducted on single and multizone models. The first evaluated the effect of assuming a more diffuse informative prior distribution for intrinsic growth rate. The baseline prior assumption was that intrinsic growth rate had an offset beta distribution with mean of $\mu_R = 0.55$ with a CV = 18%. In the sensitivity analysis, the prior for R was changed to a beta distribution with a mean of $\mu_R = 0.5$ and a CV = 57%. This allowed for more deviation from the central tendency of the prior distribution in the estimation process. This analysis was applied to the MHI models 1 and 4 and to the multizone model 6.

The second sensitivity analysis examined the effect of choosing a lower initial proportion of carrying capacity for the MHI. The baseline prior assumption for the initial proportion of K in 1948 was that $P_1 = 1.0$. Similarly, the initial values of P_T for $T > 1$ were set to be: $P_T = 0.9$ for 1948–1977, $P_T = 0.75$ for 1978–1987, and $P_T = 0.5$ for 1988–2004. In the sensitivity analyses, the initial proportion of K and the initial values of P_T for $T > 1$ were set to be one-half of the baseline value. This change was applied to the MHI models 1 and 4 and to the multizone model 6 to see if model results were affected by prior assumptions about the initial biomass of the bottomfish complex in the MHI, which was subject to fishing prior to 1948.

Projections

Two-year projections were conducted using the best-fitting single- and multizone models. For the single-zone models, the projections were conducted only for MHI while for the multizone models, projections were conducted for the MHI, Mau, and Ho'omalu Zones.

Two single-zone projections were run: status quo H and H_{MSY}. The status quo fishing mortality projection provided stochastic biomass and catch trajectories assuming the MHI harvest rate in 2004 ($H_{2004} \approx 0.43$) was realized in 2005–2006. The H_{MSY} projection provided biomass and catch trajectories assuming that an immediate reduction to H_{MSY} was realized in 2005–2007. The reduction to H_{MSY} in the MHI would be about 18% below H_{2004}.

Similarly, two multizone projections were run: status quo H, and H_{MSY}. The F status quo projection assumed that the H_{2004} values were realized in each zone during 2005–2006; these values were $H_{2004} \approx 0.43$ in the MHI, $H_{2004} \approx 0.13$ in the Mau Zone, and $H_{2004} \approx 0.06$ in the Ho'omalu Zone. Under the H_{MSY} projection, it was assumed that the harvest rate in the MHI was equal to H_{MSY} during 2005–2006 and remained equal to the H_{2004} value in the Mau and Ho'omalu Zones. As in the single-zone projections, the multizone projections provided stochastic outcomes for biomass and catch in each fishing zone.

RESULTS

MHI Models

For each of the four single-zone MHI models, the Brooks-Gelman-Rubin diagnostic indicated that the MCMC chains had converged to the posterior distribution. Plots of the BGR statistics for model 1, the most likely model (see below) were typical (Fig. 6). The BGR approached unity for each parameter (*R*, *K*, *M*, *Q*, *and P1*) and the RMSE indicating convergence was achieved.

The RMSE diagnostic was smallest for model 1 (Table 2.1), indicating that this model provided the best fit to the CPUE data. The residual patterns of the four alternative models were generally similar (Figs. 7 and 8), which was reinforced by the moderate differences in RMSE. The block of positive residuals in the early 1950s suggested that the model structure may not be appropriate for that time period. The mismatch between observed and predicted CPUE at the start of the assessment horizon suggested that aggregate bottomfish parameters or process dynamics changed in the mid-1950s. Although there was a consistent negative time trend in the residuals across models, this trend was not significantly different from 0 ($P > 0.2$) based on robust regression analyses (Rousseeuw and Yohai, 1984; S-PLUS, 2001).There was also an apparent time trend in the magnitude of negative residuals (Fig. 7), especially for models 3 and 4. This pattern suggested that model structure did not fully account for some temporal changes in the fishery CPUE series. Otherwise, the residuals appeared to have a more or less random pattern of positive and negative values across models (Fig. 7) and indicated a reasonable fit, at least from the 1960s to the present.

Parameter estimates were also similar among the four models (Table 2.1). Estimates of catchability ranged from $2.2 \cdot 10^{-4}$ to $2.5 \cdot 10^{-4}$ with CVs of 7–9%. Estimates of intrinsic growth rate ranged from 0.68 to 0.75, roughly a 10% percent difference from maximum to minimum, and had CVs of 7–9%. The range of carrying capacity estimates was 3095 to 3507 thousand pounds (13% difference) with CVs of 6–7%. The initial proportion of carrying capacity in 1948 ranged from 0.93 to 1.03 (11% difference) with CVs of 10–11%. The production shape

parameter was estimated to be between 1.11 and 1.48 (33% difference) with CVs of 20-25%. The most variable parameter across models was the production shape parameter which had the largest differences among models and the highest CVs. In contrast, the least variable parameter across models was the intrinsic growth rate.

The error variance (nuisance) parameters were also similar among models. The process error variance ranged from 0.38 to 0.48 (26% difference) with CVs of 31–32%. Similarly, the observation error variance was between 0.11 and 0.13 (18% difference) with CVs of 64–77%. The ratios-of-means of process error to observation error were between 3.4 and 4.4. This indicated that the lack of fit to the production function dynamics was 3- to 4-fold greater than the lack of fit to the CPUE indices.

Akaike information criteria of the MHI models were compared to discern the most probable model given the data. Since model 2 used distributions of annual catch data that were greater than the nominal values used in the other models, it was not compared to the other models using AIC. Of the three remaining models, model 1 provided the best fit to the MHI data with a model probability of 0.62 (Table 3.1). Model 1 was about 100-fold more likely than model 3 and almost 2-fold more likely than model 4 based on the evidence ratios (Table 3.1).

Parameter estimates from the best-fitting model were moderately correlated ($\rho < 0.4$) with two exceptions. The intrinsic growth rate (R) and the production shape parameter (M) had a strong negative correlation ($\rho = -0.51$). Similarly, the carrying capacity (K) and catchability (Q) had a very strong negative correlation ($\rho = -0.81$).

MSY-related parameter estimates were generally similar across models (Table 3.1). Estimates of B_{MSY} for MHI based on the mean value of the posterior distribution ranged from 1640 to 1767 thousand pounds with a model-averaged estimate of 1683 thousand pounds. The model-averaged B_{MSY} estimate was about 6% higher than the current estimate of 1593 thousand pounds in Moffitt et al. (2006). The estimates of MSY ranged from 627 to 679 thousand pounds. The model-averaged MSY estimate was about 76% higher than the current estimate. The MSY harvest rate estimates averaged 0.38 for the models included in the averaging. As such, the model-averaged estimate of H_{MSY} was about 67% above the current estimate of $H_{MSY} = 0.23$. Overall, the model estimates of B_{MSY} were similar to the current estimate while the model estimates of MSY and associated harvest rate were significantly higher.

Status determination criteria for the MHI bottomfish complex were evaluated within each model. Overfished status in year T was judged by the ratio of B_T to B_{MSY}. Overfishing status was measured by the ratio H_T/H_{MSY}. Plots of the trajectories of overfished and overfishing status showed a similar pattern across models. Since the evidence ratios did not strongly support a single model, the model averaged estimate of status was used to characterize the status of the MHI bottomfish complex (Fig. 9). The MHI bottomfish complex experienced a one-way trip from high biomass and low fishing mortality in the past to low biomass and high fishing mortality at present. During 1948–1981, biomass of the MHI bottomfish complex was at or above B_{MSY} and harvest rates were below H_{MSY}. In 1982,

biomass and harvest rate status changed with $B_{1982} \approx B_{MSY}$ and $H_{1982} \approx H_{MSY}$. In 1983, biomass decreased to less than B_{MSY} and harvest rate increased to more than H_{MSY}. Since then, annual biomass has remained below B_{MSY} and harvest rate has exceeded H_{MSY}. In 2004, the model-averaged biomass in the MHI was about 44% of B_{MSY} while the harvest rate was about 1.36 times H_{MSY}. As a result, in 2004 the MHI bottomfish complex would be considered to have depressed biomass (B_{2004} less than 0.7 of B_{MSY}) and excess fishing mortality (H_{2004} less that H_{MSY}).

Archipelago Models

The BGR diagnostics indicated that all model simulations converged to the posterior distribution with the exception of model 10. In model 10, there were separate carrying capacity parameters for each zone. Nonconvergence of this model suggested that the carrying capacities of the individual zones were not identifiable without the habitat constraint. Convergence diagnostic plots for model 6, the most likely model, were typical (Fig. 10).

Model 6 had the smallest RMSE (Table 2.2) and produced the best fit to the MHI CPUE data. Residuals for the Mau and Ho'omalu Zones under model 6 appeared random (Figs. 11 and 12). The residuals for MHI under model 6 had a moderate patterning similar to the most likely single zone MHI model with a block of positive residuals in the 1950s and a suggestion of an increase in the magnitude of negative residuals in recent years. Although residuals for each zone had a moderate negative time trend, this trend was not significant ($P >$ 0.4) based on robust regression analysis (Rousseeuw and Yohai, 1984). Overall, the residuals for the best fit model indicated a reasonable, albeit noisy, fit to the CPUE data across zones.

Parameter estimates for MHI were relatively similar across the multizone MHI models (Table 2.2). The catchability estimates for the MHI ranged from 2.05 to 2.47, excluding the density-dependent estimate from model 9, with CVs of 7–8%. The intrinsic growth rate estimates were also similar across models, ranging from 0.70 to 0.75 with CVs of 7–8%. Carrying capacity estimates differed by up to 8% and ranged from 3.3 to 3.6 million pounds with CVs of 5–6%. Estimates of initial biomass in proportion to carrying capacity for the MHI were not significantly different from unity across models with CVs of 9–10%. Similarly, the production shape parameter estimates were not significantly different from unity across the three models which included this as a free parameter. This indicated that there was insufficient information to estimate production shape for the MHI. Observation and process error variance estimates were also similar across models with roughly a four-to-one ratio of process to observation error, similar to the single-zone modeling results.

The Akaike information criteria values indicated that model 6 was by far the best fitting model. The evidence ratios of model 6 to the other multizone models exceeded 500:1 and the other multizone models had model probabilities of 0.002 or less. Thus, model 6, with a constant intrinsic growth rate and the 4-period catchability assumption, was clearly the dominant model and provided the basis for the multizone model-averaged parameter estimates.

Parameter estimates for the best-fitting multizone model exhibited moderate correlation, for the most part. However, some important model parameters exhibited strong correlations. The carrying capacity estimate (K) was strongly, negatively correlated with the intrinsic growth rate estimate (ρ = - 0.54) and also exhibited strong negative correlations with catchability estimates for each of the three zones: Q_{MHI} (ρ = - 0.72), Q_{Mau} (ρ = - 0.66), and $Q_{Ho'omalu}$ (ρ = - 0.81). The catchability estimate for MHI was strongly negatively correlated with K (ρ = - 0.72) and exhibited a strong positive correlation with intrinsic growth rate (ρ = 0.61) as well as catchability estimates for the other two zones: Q_{Mau} (ρ = 0.42), and $Q_{Ho'omalu}$ (ρ = 0.57). Catchabilities for the Mau and Ho'omalu Zones were also strongly positively correlated (ρ = 0.56). Last, the estimate of initial proportion of carrying capacity and the root mean squared error for the Ho'omalu Zone were strongly positively correlated (ρ = 0.66). Overall, estimates of several parameters covaried substantially for the best-fitting multizone model indicating that some parameter pairs were not well identified given the data.

Model-averaged estimates of B_{MSY} for the three zones and the Archipelago (Tables 3.2.1-3.2.4) were about 3% higher than the estimates of Moffitt et al. (2006). Given that the CVs of the model-averaged estimates were about 6%, there was no significant difference between the estimates of zonal carrying capacities from this study and Moffitt et al. (2006). In contrast, model-averaged estimates of MSY and H_{MSY} were about 50% higher than in Moffitt et al. (2006) across all three zones and the Archipelago. The substantial difference between the MSY and H_{MSY} estimates derives from the magnitude of the difference in intrinsic growth rates between this study and Moffitt et al. (2006).

Status determination criteria for the MHI from the multizone models showed the same pattern as in the single zone results. The MHI bottomfish complex experienced a one-way trip from high biomass in the 1950s–1970s to low biomass in the 1990s–2000s (Fig. 13). The model-averaged biomass for the MHI in 2004 was about 53% of B_{MSY} while the harvest rate in 2004 was about 1.21 times H_{MSY}. Thus, in 2004 the MHI bottomfish complex would be considered to have depressed biomass (B_{2004} less than 0.7 of B_{MSY}) and experiencing excess fishing mortality (H_{2004} less than H_{MSY}) if assessed as a separate management unit.

In contrast, although the Mau and Ho'omalu Zones both show decreased biomass from 1988 to 2004 (Figs. 14 and 15), biomass in both zones remains well above B_{MSY}. In 2004, model-averaged estimates of the biomasses in the Mau and Ho'omalu Zones were 64% and 69% above B_{MSY}. Similarly, the harvest rate estimates for the Mau and Ho'omalu Zones have not exceeded H_{MSY} during 1988–2004. In 2004, the model-averaged estimates of harvest rate in the Mau and Ho'omalu Zones were 38% and 18% of H_{MSY}. As a result, the Mau and Ho'omalu Zone bottomfish complexes would not be considered to have depressed biomass nor experiencing excess fishing mortality in 2004.

Status determination criteria for the entire Archipelago are available since 1988 (Fig. 16). Model-averaged estimates of biomass and harvest rate status for the Archipelago, calculated on the basis of the bottomfish habitat fractions by zone, indicate that relative biomass has declined since 1988 but still remains above B_{MSY}. In particular, Archipelago biomass was estimated to be 17% above B_{MSY} in 2004. Relative harvest rate has also declined since 1988 and was estimated to be about 67% of H_{MSY} in 2004. This indicates that the

Archipelago would not be considered to have depressed biomass and was not experiencing excess fishing mortality in 2004.

Environmental Forcing

SSH anomalies exhibited strong negative correlations with bottomfish CPUE residuals in the MHI and the Mau Zone (Figs. 17 and 18). There was also a moderate negative correlation between SSH anomalies and CPUE residuals for the Ho'omalu Zone (Fig. 19). Thus, there was a consistent pattern of negative association between SSH anomalies and CPUE residuals in recent years. It is unknown whether this pattern is consistent prior to and subsequent to the period examined (1993–2000). Regardless, this finding suggests that the fit of bottomfish production models might be improved with the additional of a structural component to represent the effect of SSH anomalies on CPUE.

Sensitivity Analyses

The sensitivity analysis for the prior distribution of the intrinsic growth rate showed that assuming a higher CV significantly increased the mean of the posterior distribution for R (Table 4). Intrinsic growth rate estimates for the most likely MHI models increased by 21–29% from the baseline model. The increased estimates of R indicated that the informative prior on intrinsic growth rate with a mean of 0.55 had the effect of constraining R to be lower than indicated by the CPUE data. In contrast, the effects of the informative prior for R on posteriors of carrying capacity, initial proportion of carrying capacity, and the current proportion of carrying capacity for MHI were not significant relative to the variability in the baseline estimates. Overall, the sensitivity results indicated that the intrinsic growth rate estimate of MHI was reduced by the informative prior on R.

The sensitivity analysis of the lower prior mean for the initial proportions of MHI carrying capacity showed that assuming a lower mean did not substantially affect the results (Table 4). Although the lower prior mean assumption reduced the estimates of initial and current proportions of K, the reductions were not significant in comparison to the variability in the baseline estimates. Thus, the model results were only moderately affected by the assumed initial proportions of carrying capacity. This also suggested there was insufficient information to estimate the initial proportion of carrying capacity even if it was significantly different than unity.

Projections

Model-averaged projections for MHI under the single-zone models show that the relative biomass status would be expected to improve under H_{MSY} scenario by about 7% from 2005 to 2006 with $B_{2006}/B_{MSY} = 0.54$ (Fig. 20). In contrast, biomass status would be expected to improve by only 1% under the status quo fishing mortality scenario, an amount that is not significantly different from 0. Similarly, catches under the H_{MSY} scenario would increase by

about 14% (+ 42,000 lbs) from 2005 to 2006 in comparison to about 2% (+ 7,000 lbs) under the status quo scenario (Fig. 20). Thus, the H_{MSY} scenario provides a larger improvement in relative biomass status and catch.

Projections for MHI under the best-fitting multizone model show similar results to the single-zone model-averaged results (Fig. 21). Relative biomass status and catch would improve by about 8% during 2005–2006 under the H_{MSY} scenario $B_{2006}/B_{MSY} = 0.66$ and 4% under the status quo scenario. In this case, there is a larger improvement for the status quo scenario under the multizone model due to correlation among parameters across zones. Regardless, the H_{MSY} scenario provides a larger relative increase in biomass and catch during 2005–2006.

DISCUSSION

Based on the hypothetical results of applying the alternative production modeling approach, the current status of the Hawaiian bottomfish complex differs by fishing zone. In the MHI, bottomfish would be considered overfished and experiencing overfishing if assessed as a separate management unit. This conclusion is consistent for the individual single- and multizone modeling results as well as for the model-averaged results. Thus, the current status of the MHI bottomfish complex is robust to model uncertainty over the set of models that were examined in this study. Nonetheless, the current status of the MHI bottomfish complex is less optimistic under the single-zone versus the multizone models. The single-zone results indicate that current fishing mortality is 36% above the overfishing threshold while the multizone model results suggest that F_{2004} was only 21% above the threshold. This difference in status estimation arises because the multizone model parameters are correlated when the CPUE data are fit simultaneously in the three fishing zones. Similarly, the single-zone results indicate that biomass in 2004 was 44% of B_{MSY} versus 53% for the multizone models. Overall, the results suggest that fishing mortality needs to be reduced by at least 21% and possibly by twice that amount to eliminate excess fishing mortality in the MHI. Similarly, biomass needs to be rebuilt by about twofold to lie within the probable range of B_{MSY}. While the multizone results are more consistent with the operating hypothesis that there is sufficient interchange of larvae and/or adult fish across zones to justify joint estimation of parameters, it would be prudent to consider the ramifications if this assumption is not correct.

In contrast, bottomfish in both the Mau and Ho'omalu Zones would not be considered overfished nor experiencing overfishing. In 1990, bottomfish of the Mau Zone were being harvested below but near the overfishing threshold. Since then, F has been reduced and has remained less than 50% of H_{MSY} in recent years. Biomass in the Mau Zone has not fallen below the overfished threshold during 1988–2004 and is currently over 50% above B_{MSY}. Similarly, it appears that the Ho'omalu Zone bottomfish complex has never been close to experiencing overfishing or being in an overfished status during 1988–2004. Currently, the Ho'omalu Zone bottomfish are being harvested at less than 20% of H_{MSY} while Ho'omalu Zone biomass is more than 50% above B_{MSY}. Thus, the Mau and Ho'omalu Zone bottomfish stocks would have to be considered healthy and lightly exploited, particularly in comparison to the MHI bottomfish complex.

Given the current healthy status of bottomfish in the Mau and Ho'omalu Zones, the overall status of bottomfish in the Archipelago as a whole is also positive. Harvest rates are currently two-thirds of the overfishing threshold, and biomass is over 15% above B_{MSY}. It also appears that the Archipelago has not been overfished during the 1988–2004 assessment time horizon, although harvest rates approached or were at the overfishing threshold in the 1990s. While bottomfish on an Archipelago-wide basis are currently not overfished or experiencing overfishing according to the results of this study, it should be noted that this evaluation is contingent on the assumption that the linkage among bottomfish in the three zones is relatively strong and consistent through time.

Constant catchability models provided the best fit to the single-zone data for MHI. The best-fitting single-zone models had a constant Q but also included the shape parameter for the surplus production curve. However, the point estimate of the shape parameter was not significantly different from 1, suggesting that the inclusion of the shape parameter may have been aliasing another effect related to the decreasing abundance of MHI bottomfish throughout the time series. One such potential effect would be increasing catchability. Regardless, the model selection criterion suggested that either catchability changes through time were minor or not detectable within the single-zone modeling context. Constant catchability seems plausible since the commercial bottomfish fishery has operated with similar handline gear since the 1950s (Haight et al., 1993). Although the design of the hooks, bait, and gear deployment methods have not changed much if at all, the use of powered reels, modern navigational equipment, and fish finders has likely increased fishing power through time. However, other factors are likely to have affected overall bottomfish catchability in an unknown manner. For example, changes in the species composition of the bottomfish complex may have reduced or increased catchability through time. Similarly, changes in the composition of the fishing fleet and the relative experience of fishermen could have reduced or increased catchability on average. Nonetheless, it seems likely that there was some increase in relative fishing power although it was not detected in the single-zone models.

In contrast, the 4-period increasing catchability model clearly provided the best fit to the multizone CPUE data and was by far the most likely model. This model incorporated the assumption that catchability had increased based on changes in the fishery and fishing gear as in Moffitt et al. (2006). In comparison, the alternative multizone models that assumed constant or density-dependent catchability received relatively little support from the data and were highly improbable.

One technical concern about the current bottomfish assessment is that the CPUE data provide limited information on resource productivity because of the characteristic one-way trip from high to low biomass with no return to high biomass (see, for example, Hilborn and Walters, 1992). Based on the parameter correlations, the biomass scaling parameters of carrying capacity and fishery catchability have strong negative correlations for the single- and multizone models. This effect might be expected since an increasing catchability implies a lower biomass for fixed CPUE. Regardless, the carrying capacity estimate for MHI had consistent values across alternative models. The carrying capacities of the Mau and Ho'omalu Zones, in contrast, did not appear to be identifiable since the Bayesian MCMC simulations

did not converge when the carrying capacities were free parameters. This lack of identifiability is not surprising given the correlations between *K* and *Q* and the short time series for the Mau and Ho'omalu Zones. In contrast, comparing estimates of parameters for MHI under the single- and multizone modeling approaches suggests that the carrying capacity estimate is relatively robust in the inclusion of multizone CPUE data.

In contrast to the carrying capacity parameter, it appears that the intrinsic growth rate parameter could be freely estimated for each zone. This is important because the intrinsic growth rate of the bottomfish complex might be expected to vary given the substantial latitudinal differences among fishing zones. It is interesting that intrinsic growth rate estimates by fishing zone showed a cline from a low in the Ho'omalu Zone to a high in MHI. This cline may reflect average physical transport of bottomfish larvae under the general northwest to southeast current flow in the Archipelago. Recent research by Kobyashi using simulations of circulation models for the region (pers. comm., unpublished manuscript) suggests that one might expect higher larval retention in MHI, and hence a potentially higher intrinsic growth rate.

The shape parameter of the power function surplus production curve does not appear to be essential for the multizone models. This also held true for the single-zone models in the sense that when the shape parameter was freely estimated, it was not significantly different from 1.0. This supports the assumption that a Schaefer production model, as in the current assessment, is reasonable for the Hawaiian bottomfish data despite controversy over the appropriateness of this simple model (Maunder, 2004; Praeger, 2004). It remains to be seen whether future work will show that a skewed production curve is more appropriate for Hawaiian bottomfish.

Estimation of the initial proportion of carrying capacity is hampered by a lack of auxiliary information on likely values of this parameter across the three fishing zones. In any case, fitting the CPUE data did not alter the prior assumption that the complex was fluctuating near carrying capacity. This indicates that there was little or no information in the CPUE data to adjust the prior assumption. While it may be appropriate to consider the bottomfish resource of MHI to be fluctuating near carrying capacity at the beginning of the assessment time horizon in 1948, it is clear that this assumption is questionable for the Mau and Ho'omalu Zones in 1988. Although the NWHI zones have experienced much lower exploitation rates than MHI, the bottomfish stocks in the NWHI zones were likely fished to more productive levels below carrying capacity by the mid-1980s.

The effect of overestimating the initial proportion of carrying capacity on estimated trends in biomass and fishing mortality may be moderate since there was a lack of strong correlation between the estimates of initial proportion of carrying capacity for the MHI and Mau Zones. The Ho'omalu Zone initial proportion of carrying capacity was strongly correlated with the goodness of fit suggesting that it was potentially important for this zone. Sensitivity analyses using an informative prior on initial proportion of carrying capacity suggested it had a weak influence on most parameter estimates. Overall, it appeared that overestimating the initial proportion of carrying capacity altered the overall scale of trends in biomass and fishing mortality but did not affect their relative trends.

Results from the Bayesian surplus production modeling approach were generally similar to those of Moffitt et al. (2006). Estimates of biomass and fishing mortality trends were consistent across modeling approaches. The results indicated higher intrinsic growth rates and this led to higher estimates of MSY and H_{MSY}. In particular, the overfishing threshold would increase by about 40–50% based on the model-averaged results. In comparison, the estimates of carrying capacity were very similar to those in Moffitt et al. (2006) indicating that target biomasses (B_{MSY}) were unaffected by differences in the modeling approach. Given the potential for strong correlation between carrying capacity and intrinsic growth rate under the Bayesian estimation approach, estimates of reference points warrant a cautious interpretation. For example, if carrying capacity (and hence B_{MSY}) is underestimated, then intrinsic growth rate (and hence H_{MSY}) is likely being overestimated. Such a scenario could occur, for example, if the recreational bottomfish catch is substantial in comparison to commercial catch but recreational catch is not included in the surplus production model. Overall, the use of precautionary total allowable catch adjustments, as recommended in Restrepo et al. (1998) would be a prudent management approach given the uncertainty in biological reference points.

The use of diffuse priors for intrinsic growth rate led to estimates that were higher than those obtained with an informative prior. This increase in the estimated intrinsic growth rate suggests that the CPUE and reported catch data are not entirely consistent with the informative prior mean for intrinsic growth rate. This mismatch could occur because a higher growth rate would be needed to account for the observed catch relative to changes in CPUE. Overall, the effect of not including recreational catch will be to underestimate the potential productivity of the bottomfish resource, as suggested in the sensitivity analyses of the effect of misreported catch and the hypothetical recreational to commercial catch ratio.

The potential importance of environmental forcing on bottomfish was suggested by the negative correlations of SSH anomalies with CPUE residuals in each of the regions. Although the actual biological response is unknown, the correlated residual patterns could arise from at least two sources. First, the pattern could be the direct result of changes in food availability for bottomfish. In particular, the increase in bottom-up productivity that arises when SSHs are relatively low because of increased upwelling and current divergence could increase the amount of zooplankton and other small nekton available to snappers that consume zooplankton (Haight et al., 1993). Second, changes in productivity as indexed by SSH anomalies may alter the depth or spatial distribution of bottomfish as they forage. If this behavioral effect was consistent across species through time it could alter bottomfish catchability coefficients and lead to differences between observed and model predictions of CPUE. Regardless of the mechanism, it would be useful to extend the time frame of the SSH analysis to better understand the nature and extent of the apparent coupling.

If fishery-dependent and fishery-independent data collection systems for Hawaiian bottomfish could be augmented, then it seems likely that age- or length-structured assessment models could be applied to assess individual bottomfish species. The first priority in this context would be to sample the existing recreational fishery operations so as to estimate the total recreational catch as well as the length composition by species. The collection of length

composition and length-weight measurements from the Honolulu fish auction would provide direct information on commercial fishery removals with only a minor, if any, effect on the quality of fish offered for sale. Such data could be used to evaluate the catch at age by species given sufficient age-length keys and ongoing sampling effort. The collection of age samples (otoliths) and food habits (stomachs) data is more challenging because it would require invasive sampling of individual fish. Nonetheless, this information is crucial to estimating life history parameters and characterizing the strength of biological interactions among bottomfish species. In any case, to enable analysis of spatial variability, it will be important to obtain georeferenced data to be able to accurately identify where samples of fish were caught. In particular, being able to identify the location of catch, length frequency, stomach, and otolith samples would greatly enhance the use and interpretation of such data in relation to existing and planned bottomfish restricted fishing areas as well as essential fish habitat. Last, the development of a consistent fishery-independent survey of Hawaiian bottomfish would greatly enhance the capacity to assess and manage these resources.

The effects of using a more formal statistical approach to fit bottomfish surplus production models were moderate but important in some cases. In particular, the status determination criteria estimates from these models were, for the most part, consistent with the current assessment although the overall status of the Archipelago differed. In technical terms, the most direct consequence of using the Bayesian surplus production models was that parameter uncertainty can be directly estimated. This is an important feature if fishery management incorporates analyses of risk or if precautionary adjustments are used to buffer against uncertainty in a data-limited situation. The use of risk analyses seems likely given that the MHI bottomfish complex has depressed biomass and is experiencing excess fishing mortality. In addition, the application of model averaging appears to be very useful in this setting because it allows for alternative model structures to be evaluated and results to be melded together in an objective manner. For the single-zone main Hawaiian Islands scenario, there was some model ambiguity and the use of model-averaged estimates provided a clear way to describe results. In contrast, the multizone model comparison indicated that there was really only one model that provided the best fit to the data. In this case, the use of the single best-fitting model was appropriate, conditioned on the typical caveats associated with interpreting any quantitative stock assessment (e.g., Koeller, 2003).

ACKNOWLEDGMENTS

The altimeter products were produced by Salto/Duacs and distributed by AVISO, with support from CNES and special thanks to Dave Foley.

REFERENCES

Brooks, S. P., and A. Gelman.
1998. Alternative methods for monitoring convergence of iterative simulations. Journal of Computational and Graphical Statistics, 7:434–455.

Burnham, K. P., and D. R. Anderson.
2002. Model selection and multimodel inference, 2nd edition. Springer Verlag, New York, 488 pp.

Congdon, P.
2001. Bayesian statistical modeling. Wiley, New York, 531 pp.

Ducet, N., P. Y. Le Traon, and G. Reverdin.
2000. Global high resolution mapping of ocean circulation from the combination of Topex/Poseidon and ERS-1/2. J. Geophys. Res. 105(C8), 19477–19498.

Gilks, W. R., S. Richardson, and D. J. Spiegelhalter. [Eds.]
1996. Markov Chain Monte Carlo in Practice. Chapman and Hall, London. 486 pp.

Haight, W. R., D. R. Kobyashi, and D.E. Kawamoto.
1993. Biology and management of deepwater snappers of the Hawaiian Archipelago. Mar. Fish. Rev. 55:20–27.

Hamm, D., and K. Lum.
1992. Preliminary results of the Hawaii small-boat fisheries survey. Honolulu Lab., Southwest Fish. Sci. Cent., Natl. Mar. Fish. Serv., NOAA, Honolulu, HI 96822-2396. Southwest Fish. Sci. Cent. Admin. Rep. H-92-08, 35 p.

Hilborn, R., and C. Walters.
1992. Quantitative fisheries stock assessment. Chapman and Hall, New York, 570 pp.

Koeller, P.
2003. The lighter side of reference points. Fish. Res. 62:1–6.

Maunder, M.
2003. Is it time to discard the Schaefer model from the stock assessment scientist's toolbox? Fish. Res. 61:145–149.

Martinez-Andrade, F.
2003. A comparison of life histories and ecological aspects among snappers (Pisces: Lutjanidae). Ph.D. Dissertation, Louisiana State Univ. 194 p.

McAllister, M. K., E. K. Pikitch, and E. A. Babcock.
2001. Using demographic methods to construct Bayesian priors for the intrinsic rate of increase in the Schaefer model and implications for stock rebuilding. Can. J. Fish. Aquat. Sci. 58:1871–1890.

Meyer, R., and R. Millar.
1999. BUGS in Bayesian stock assessments. Can. J. Fish. Aquat. Sci. 56: 1078–1086.

Moffitt, R., D. Kobayashi, and G. Dinardo.
2006. Status of the Hawaiian bottomfish stocks, 2004. Pacific Islands Fish. Sci. Cent., Natl. Mar. Fish. Serv., NOAA, Honolulu, HI 96822-2396. Pacific Islands Fish. Sci. Cent. Admin. Rep. H-06-01, 45 p.

Praeger, M. P.
2003. Reply to the letter to the editor by Maunder. Fish. Res. 61:151–154.

Restrepo, V. R., G. G. Thompson, P. M. Mace, W. K. Gabriel, L. L. Low, A. D. MacCall, R. D. Methot, J. E. Powers, B. L. Taylor, P. R. Wade, and J. F. Witzig.
1998. Technical guidance on the use of precautionary approaches to implementing national standard 1 of the Magnuson- Stevens fishery conservation and management act. NOAA Technical Memorandum NMFS F/SPO.

Rousseeuw, P., and V. Yohai.
1984. Robust regression by means of S-estimators. In Robust and Nonlinear Time Series Analysis, J. Franke, W. Hardle, and R. Martin (Eds.). Lecture Notes in Statistics, 26:256–272. Springer Verlag, New York.

Spiegelhalter, D., A. Thomas, N. Best, and D. Lunn.
2003. WinBUGS User Manual. Available at: http://www.mrc.bsu.carn.ac.uk/bugs/winbugs/manual14.pdf

S-PLUS
2001. S-PLUS 6 for windows guide to statistics, volume 1. Insightful Corporation, Seattle, WA.

Table 1.--Hawaiian bottomfish species used for production model analyses from Moffitt et al. (2006).

Common name	Local name	Scientific name
Pink snapper	Opakapaka	*Pristipomoides filamentosus*
Longtail snapper	Onaga	*Etelis coruscans*
Squirrelfish snapper	Ehu	*Etelis carbunculus*
Sea bass	Hapuupuu	*Epinephelus quernus*
Grey jobfish	Uku	*Aprion virescens*
Snapper	Gindai	*Pristipomoides zonatus*
Snapper	Kalekale	*Pristipomoides sieboldii*
Yelloweye snapper	Yelloweye opakapaka	*Pristipomoides flavipinnis*
Blue stripe snapper	Taape	*Lutjanus kasmira*
Yellowtail snapper	Yellowtail kalekale	*Pristipomoides auricilla*
Silver jaw jobfish	Lehi	*Aphareus rutlians*
Amberjack	Kahala	*Serioila dumerili*
Thick lipped trevally	Butaguchi	*Pseudocaranx dentex*
Giant trevally	White ulua	*Caranx ignoblis*
Black jack	Black ulua	*Caranx lugubris*
Armorhead		*Pseudopentaceros richardsoni*

Table 2.1.--Summary of the mean of the posterior distribution of main Hawaiian Islands (MHI) bottomfish surplus production model parameter estimates and the standard error (in parentheses) for models that were fit to only the MHI catch-per-unit-effort (CPUE) data as well as estimates of harvest rate (H_{2004}/H_{MSY}) and biomass (B_{2004}/B_{MSY}) status determination criteria in 2004.

Model description	RMSE for MHI CPUE fit	MHI Catchability (Q)	MHI Intrinsic Growth Rate (R)	MHI Carrying Capacity (K, 000s of lbs)	MHI Initial Proportion of K (P_1)	MHI Shape Parameter (M)	MHI Process Error Variance (η^2)	MHI Observation Error Variance (υ^2)	MHI Harvest Rate Ratio in 2004 (H_{2004}/H_{MSY})	MHI Biomass Ratio in 2004 (B_{2004}/B_{MSY})
Model (1) Lognormal process & observation error; power function dynamics; constant Q	0.098 (0.031)	2.20E-04 (1.87E-05)	0.68 (0.06)	3095 (218)	0.94 (0.09)	1.34 (0.30)	0.038 (0.012)	0.011 (0.007)	1.18 (0.14)	0.50 (0.06)
Model (2) Same as (1) with uniform catch error 1948–89,1990–04	0.102 (0.036)	2.17E-04 (1.82E-05)	0.68 (0.06)	3154 (226)	0.93 (0.08)	1.48 (0.37)	0.041 (0.013)	0.012 (0.009)	1.13 (0.14)	0.49 (0.06)
Model (3) Same as (1) but uses 4-period Q submodel from AR-06-01	0.107 (0.035)	2.50E-04 (2.02E-05)	0.74 (0.06)	3476 (217)	1.03 (0.10)	1.11 (0.22)	0.048 (0.015)	0.013 (0.010)	1.64 (0.21)	0.34 (0.04)
Model (4) Same as (1) but uses Schaefer dynamics instead of power function	0.101 (0.029)	2.48E-04 (1.67E-05)	0.75 (0.05)	3507 (195)	1.03 (0.10)		0.048 (0.015)	0.011 (0.007)	1.66 (0.20)	0.34 (0.04)
Model average	0.099 (0.030)	2.31E-04 (2.03E-05)	0.71 (0.07)	3252 (290)	0.97 (0.10)	1.21 (0.29)	0.042 (0.014)	0.011 (0.007)	1.36 (0.29)	0.44 (0.09)

Table 2.2.--Summary of the mean of the posterior distribution of main Hawaiian Islands (MHI) bottomfish surplus production model parameter estimates and standard error (in parentheses) for models that were fit to the MHI, Mau, and Ho'omalu Zone catch-per-unit effort data as well as estimates of harvest rate (H_{2004}/H_{MSY}) and biomass (B_{2004}/B_{MSY}) status determination criteria in 2004.

Model description	RMSE for MHI CPUE fit	MHI Catchability (Q)	MHI Intrinsic Growth Rate (R)	MHI Carrying Capacity (K, 000s of lbs)	MHI Initial Proportion of K (P_1)	MHI Shape Parameter (M)	MHI Process Error Variance (η^2)	MHI Observation Error Variance (υ^2)	MHI Harvest Rate Ratio in 2004 (H_{2004}/H_{MSY})	MHI Biomass Ratio in 2004 (B_{2004}/B_{MSY})
Model (5) Same as (4) except Mau/Ho'omalu Zone K set to be habitat fraction of MHI K, assumes a common R among zones, and uses a constant Q	0.100 (0.029)	2.44E-04 (1.68E-05)	0.737 (0.056)	3547 (194)	1.04 (0.10)		0.048 (0.015)	0.011 (0.007)	1.67 (0.20)	0.34 (0.04)
Model (6) Same as (5) but uses 4-period Q submodel for MHI from AR-06-01	0.089 (0.026)	2.05E-04 (1.63E-05)	0.703 (0.057)	3276 (200)	0.96 (0.09)		0.039 (0.011)	0.009 (0.005)	1.21 (0.14)	0.53 (0.06)
Model (7) Same as (6) but uses power function dynamics	0.101 (0.031)	2.43E-04 (2.00E-05)	0.735 (0.059)	3542 (208)	1.04 (0.10)	1.02 (0.20)	0.049 (0.015)	0.011 (0.008)	1.68 (0.21)	0.34 (0.04)
Model (8) Same as (6) but estimates a separate R for each zone	0.100 (0.029)	2.45E-04 (1.64E-05)	0.746 (0.054)	3554 (190)	1.03 (0.10)		0.047 (0.014)	0.011 (0.007)	1.65 (0.19)	0.34 (0.04)

Table 2.2. Continued.

Model description	RMSE for MHI CPUE fit	MHI Catchability (Q)	MHI Intrinsic Growth Rate (R)	MHI Carrying Capacity (K, 000s of lbs)	MHI Initial Proportion of K (P_1)	MHI Shape Parameter (M)	MHI Process Error Variance (η^2)	MHI Observation Error Variance (υ^2)	MHI Harvest Rate Ratio in 2004 (H_{2004}/H_{MSY})	MHI Biomass Ratio in 2004 (B_{2004}/B_{MSY})
Model (9) Same as (8) but assumes density-dependent catchability in MHI	0.097 (0.029)	4.17E-04 (2.15E-04)	0.714 (0.056)	3337 (195)	0.98 (0.10)		0.043 (0.014)	0.010 (0.006)	1.28 (0.18)	0.49 (0.07)
Model (10) Same as (8) but estimates K for each zone	Did not converge									
Model (11) Same as (7) but estimates a separate R for each zone	0.104 (0.031)	2.46E-04 (1.96E-05)	0.740 (0.057)	3530 (207)	1.03 (0.10)	1.06 (0.19)	0.048 (0.014)	0.012 (0.008)	1.65 0.20	0.34 (0.04)
Model (12) Same as (11) but uses power function dynamics only for MHI	0.104 (0.032)	2.47E-04 (1.99E-05)	0.736 (0.058)	3532 (206)	1.03 (0.11)	1.08 (0.21)	0.048 (0.015)	0.012 (0.008)	1.64 (0.21)	0.34 (0.04)
Model (13) Same as (8) but assumes a 3-period Q model for MHI (combines 1st & 2nd Q periods)	0.102 (0.028)	2.31E-04 (1.56E-05)	0.748 (0.052)	3464 (187)	0.99 (0.09)		0.038 (0.012)	0.011 (0.007)	1.54 (0.18)	0.37 (0.04)
Model (14) Same as (6) but includes estimate of recreational catch	0.087 (0.026)	1.808E-04 (1.23E-05)	0.770 (0.053)	3665 (192)	0.96 (0.09)		0.048 (0.014)	0.008 (0.005)	1.28 (0.14)	0.54 (0.05)

Table 3.1.--Goodness of fit of the alternative single-zone, MHI surplus production models along with mean posterior values of MSY-related reference points, model-averaged estimates and their coefficients of variation (CV) and corresponding values from Moffitt et al. (2006).

Model	AIC Difference Δ_k	Relative Likelihood	Evidence Ratio	Model Probability	B_{MSY}	MSY	H_{MSY}
1	—	1.0	1	0.619	1640	627	0.38
2	Not applicable				1700	673	0.40
3	9.2	0.010	99.5	0.006	1767	679	0.38
4	1	0.607	1.6	0.375	1753	658	0.38
Model Average					1683	639	0.38
CV					7.0%	8.5%	8.7%
Moffitt et al. (2006)					1593	362	0.23

Table 3.2.1.--Goodness of fit of the alternative multizone MHI surplus production models along with mean posterior values of MSY-related reference points, model-averaged estimates and their coefficients of variation (CV) and corresponding values from Moffitt et al. (2006).

Model	AIC Difference Δ_k	Relative Likelihood	Evidence Ratio	Model Probability	B_{MSY}	MSY	H_{MSY}
5	13.0	0.002	665	0.002	1773	652	0.37
6	—	1.000	1	0.998	1638	574	0.35
7	17.2	0.000	5432	0.000	1772	649	0.37
8	17.6	0.000	6634	0.000	1777	662	0.37
9	16.7	0.000	4230	0.000	1668	594	0.36
11	24.2	0.000	179872	0.000	1781	672	0.38
12	27.4	0.000	890911	0.000	1789	677	0.38
13	19.9	0.000	20952	0.000	1732	646	0.37
14	Not applicable				1832	705	0.38
Model Average					1638	574	0.35
CV					6.1%	7.1%	8.0%
Moffitt et al. (2006)					1593	362	0.23

Table 3.2.2.--Goodness of fit of the alternative multizone Mau Zone surplus production models along with mean posterior values of MSY-related reference points, model-averaged estimates and their coefficients of variation (CV) and corresponding values from Moffitt et al. (2006).

Model	AIC Difference Δ_k	Relative Likelihood	Evidence Ratio	Model Probability	B_{MSY}	MSY	H_{MSY}
5	13.0	0.002	665	0.002	491	181	0.37
6	-	1.000	1	0.998	454	159	0.35
7	17.2	0.000	5432	0.000	491	180	0.37
8	17.6	0.000	6634	0.000	488	135	0.28
9	16.7	0.000	4230	0.000	462	130	0.28
11	24.2	0.000	179872	0.000	493	141	0.29
12	27.4	0.000	890911	0.000	489	135	0.28
13	19.9	0.000	20952	0.000	480	134	0.28
14	Not applicable				508	195	0.38
Model Average					454	159	0.35
CV					6.1%	7.1%	8.0%
Moffitt et al. (2006)					441	100	0.23

Table 3.2.3.--Goodness of fit of the alternative multizone Ho'omalu Zone surplus production models along with mean posterior values of MSY-related reference points, model-averaged estimates and their coefficients of variation (CV) and corresponding values from Moffitt et al. (2006).

Model	AIC Difference Δ_k	Relative Likelihood	Evidence Ratio	Model Probability	B_{MSY}	MSY	H_{MSY}
5	13.0	0.002	665	0.002	1703	626	0.37
6	—	1.000	1	0.998	1573	551	0.35
7	17.2	0.000	5432	0.000	1701	623	0.37
8	17.6	0.000	6634	0.000	1692	458	0.27
9	16.7	0.000	4230	0.000	1602	436	0.27
11	24.2	0.000	179872	0.000	1707	481	0.28
12	27.4	0.000	890911	0.000	1695	460	0.27
13	19.9	0.000	20952	0.000	1663	451	0.27
14	Not applicable				1759	676	0.38
Model Average					1573	551	0.35
CV					6.1%	7.1%	8.0%
Moffitt et al. (2006)					1531	348	0.23

Table 3.2.4.--Goodness of fit of the alternative multizone Hawaiian Archipelago surplus production models along with mean posterior values of MSY-related reference points, model-averaged estimates and their coefficients of variation (CV) and corresponding values from Moffitt et al. (2006).

Model	AIC Difference Δ_k	Relative Likelihood	Evidence Ratio	Model Probability	B_{MSY}	MSY	H_{MSY}
5	13.0	0.002	665	0.002	3967	1459	0.37
6	-	1.000	1	0.998	3665	1284	0.35
7	17.2	0.000	5432	0.000	3964	1452	0.37
8	17.6	0.000	6634	0.000	3975	1259	0.32
9	16.7	0.000	4230	0.000	3730	1159	0.31
11	24.2	0.000	179872	0.000	3984	1292	0.32
12	27.4	0.000	890911	0.000	3974	1272	0.32
13	19.9	0.000	20952	0.000	3875	1231	0.32
14	Not applicable				4099	1576	0.38
Model Average					3666	1284	0.35
CV					6.1%	7.1%	8.0%
Moffitt et al. (2006)					3566	811	0.23

Table 4.--Sensitivity of parameter estimates for the most likely bottomfish surplus production models. Mean estimates for the baseline model (with percentage coefficients of variation below), along with mean estimates from model runs with the diffuse prior distribution for intrinsic growth rate (R) and with a 50% lower prior mean for the initial proportion of carrying capacity (with percent change from the baseline values in parentheses).

Bottomfish Surplus Production Model	MHI Intrinsic Growth Rate (R)	MHI Carrying Capacity (K, 000s of lbs)	MHI Initial Proportion of K (P_{1948})	MHI Current Proportion of K (P_{2004})
Model (1) Baseline	0.68 9%	3095 7%	0.94 10%	0.27 11%
Model (1) Higher CV for Prior on R	0.88 (29%)	2949 (-5%)	0.93 (-1%)	0.26 (-4%)
Model (1) 50% Lower Prior Mean on Initial Proportion of K	0.68 (0%)	3062 (-1%)	0.83 -12%)	0.25 (-7%)
Model (4) Baseline	0.74 8%	3476 6%	1.03 10%	0.17 12%
Model (4) Higher CV for Prior on R	0.93 (26%)	3196 (-8%)	0.98 (-5%)	0.17 (0%)
Model (4) 50% Lower Prior Mean on Initial Proportion of K	0.76 (3%)	3474 (0%)	0.93 (-10%)	0.17 (0%)
Model (6) Baseline	0.70 9%	3276 6%	0.96 9%	0.27 11%
Model (6) Higher CV for Prior on R	0.85 (21%)	2986 (-9%)	0.93 (-3%)	0.26 (-4%)
Model (6) 50% Lower Prior Mean on Initial Proportion of K	0.72 (3%)	3250 (-1%)	0.84 (-13%)	0.25 (-7%)

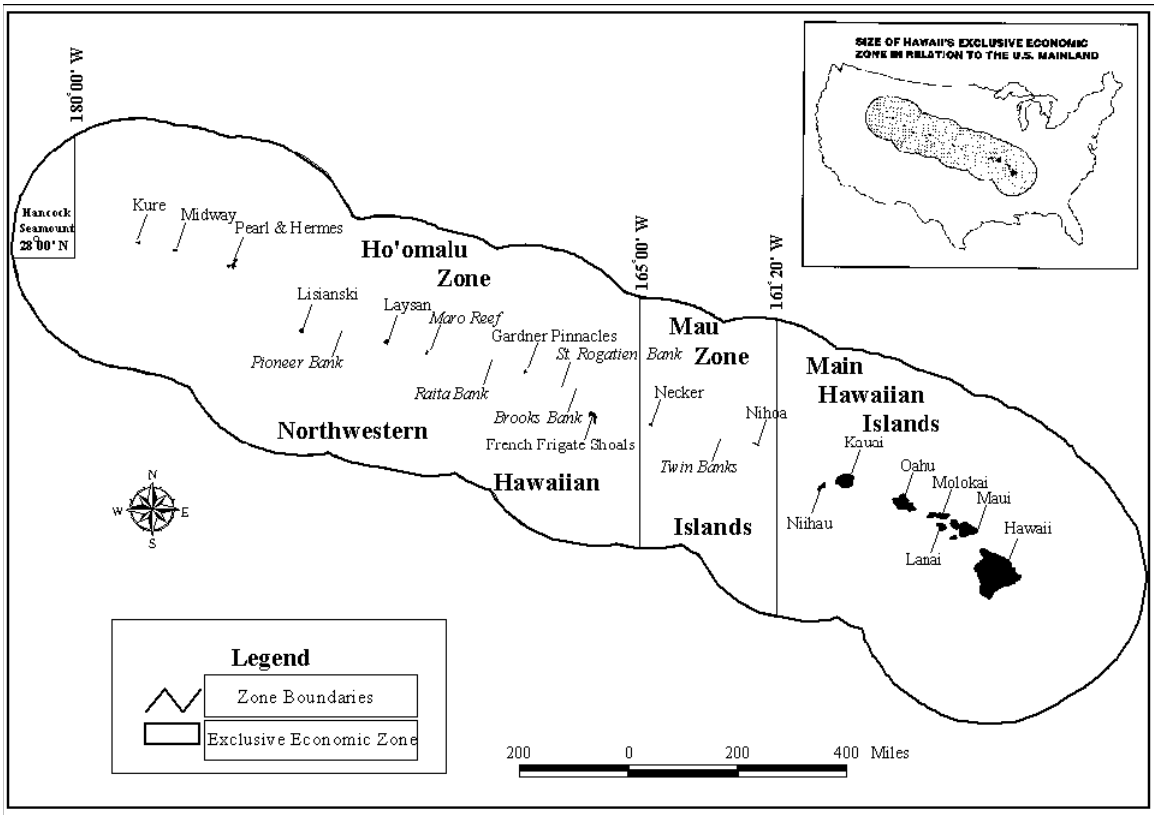

Figure 1.--Location of the Hawaiian bottomfish assessment zones: MHI, the Mau Zone, and the Ho'omalu Zone.

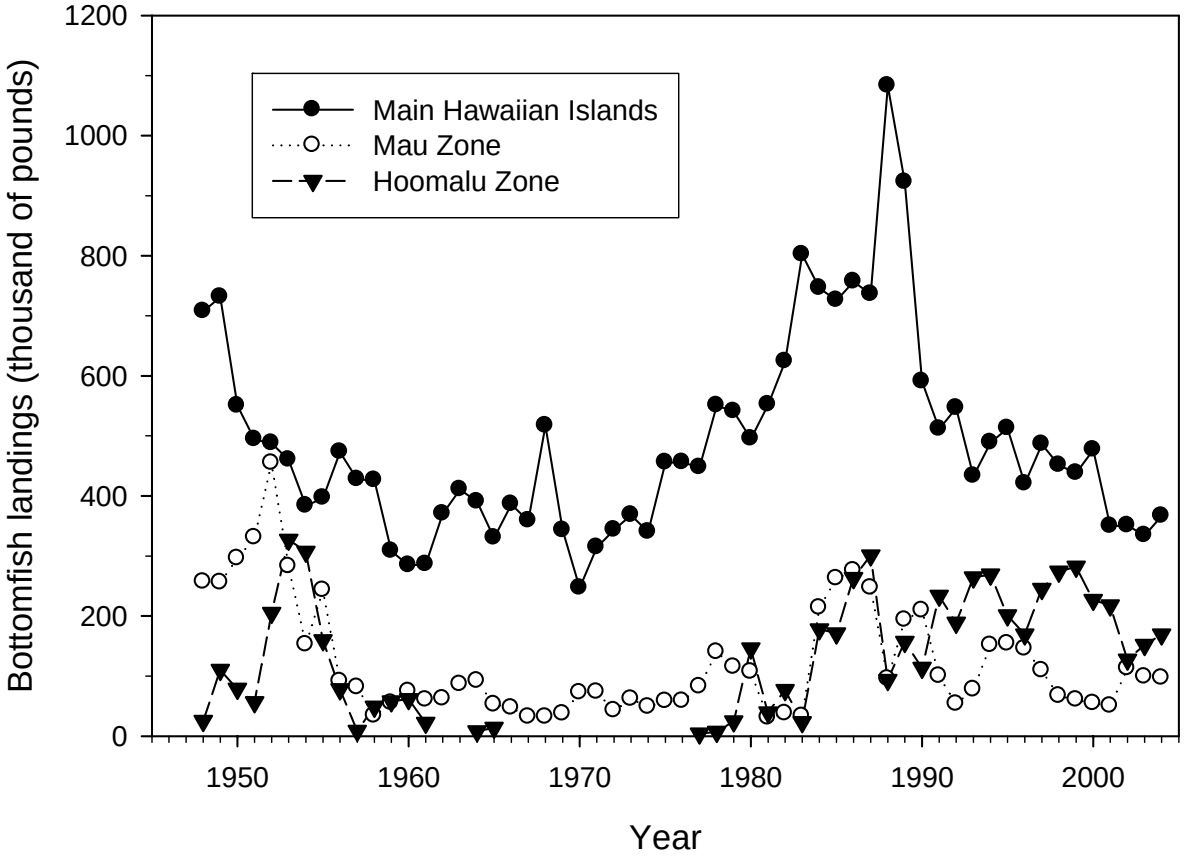

Figure 2.--Nominal commercial bottomfish landings by assessment zone, 1948-2004.

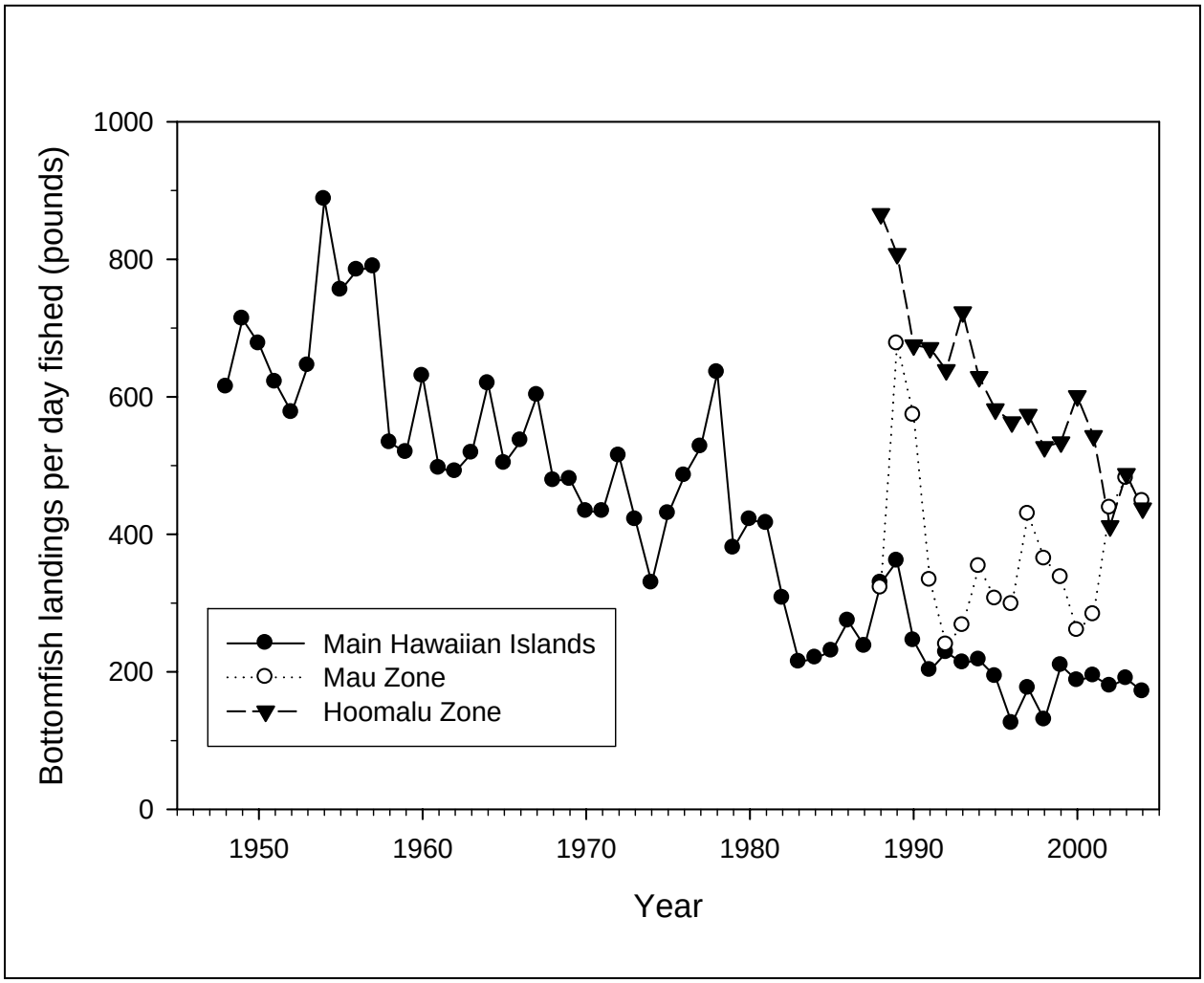

Figure 3.--Commercial bottomfish catch-per-unit-effort by assessment zone.

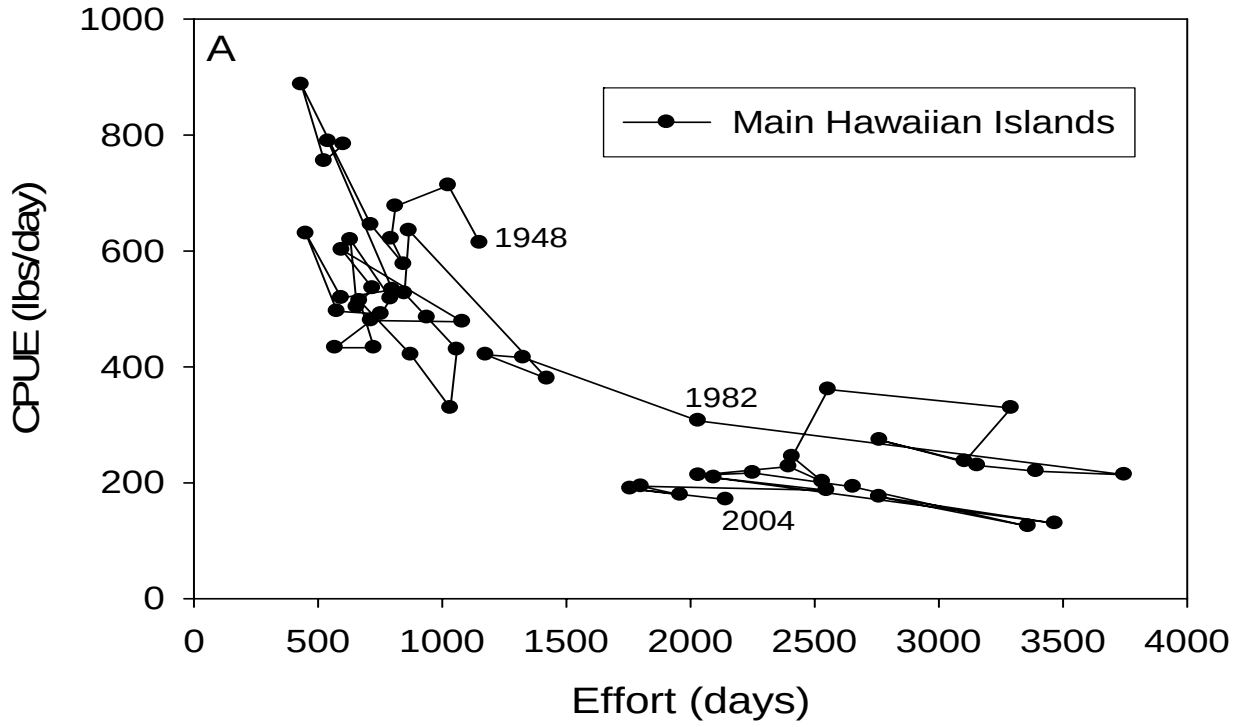

Figure 4.--Trajectories of CPUE and fishing effort for MHI (A), the Mau Zone (B), and the Ho'omalu Zone (C).

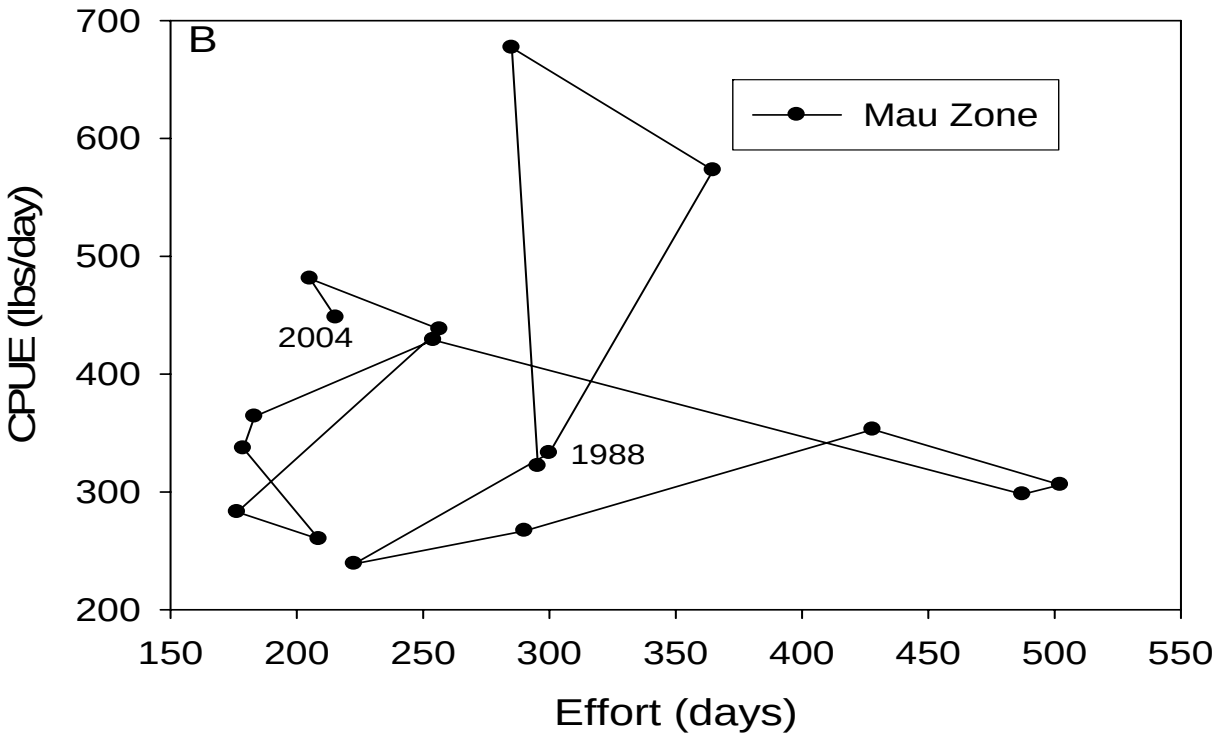

Figure 4.--Continued.

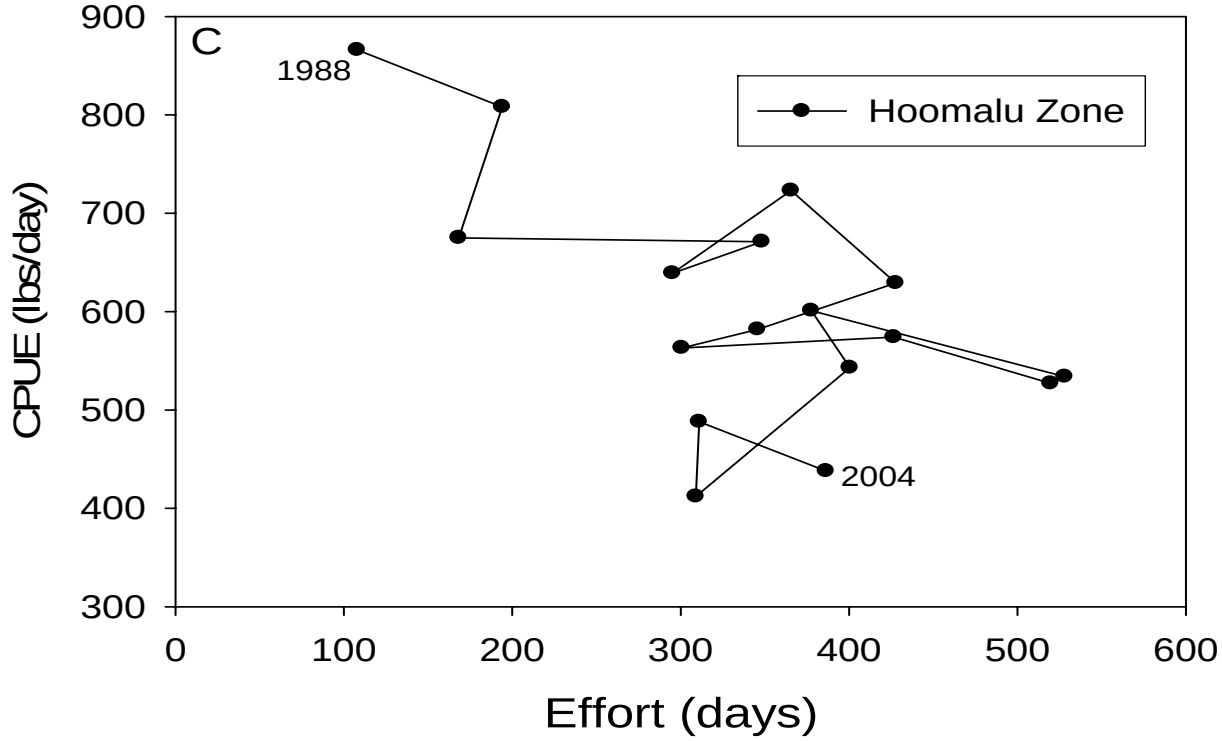

Figure 4.--Continued.

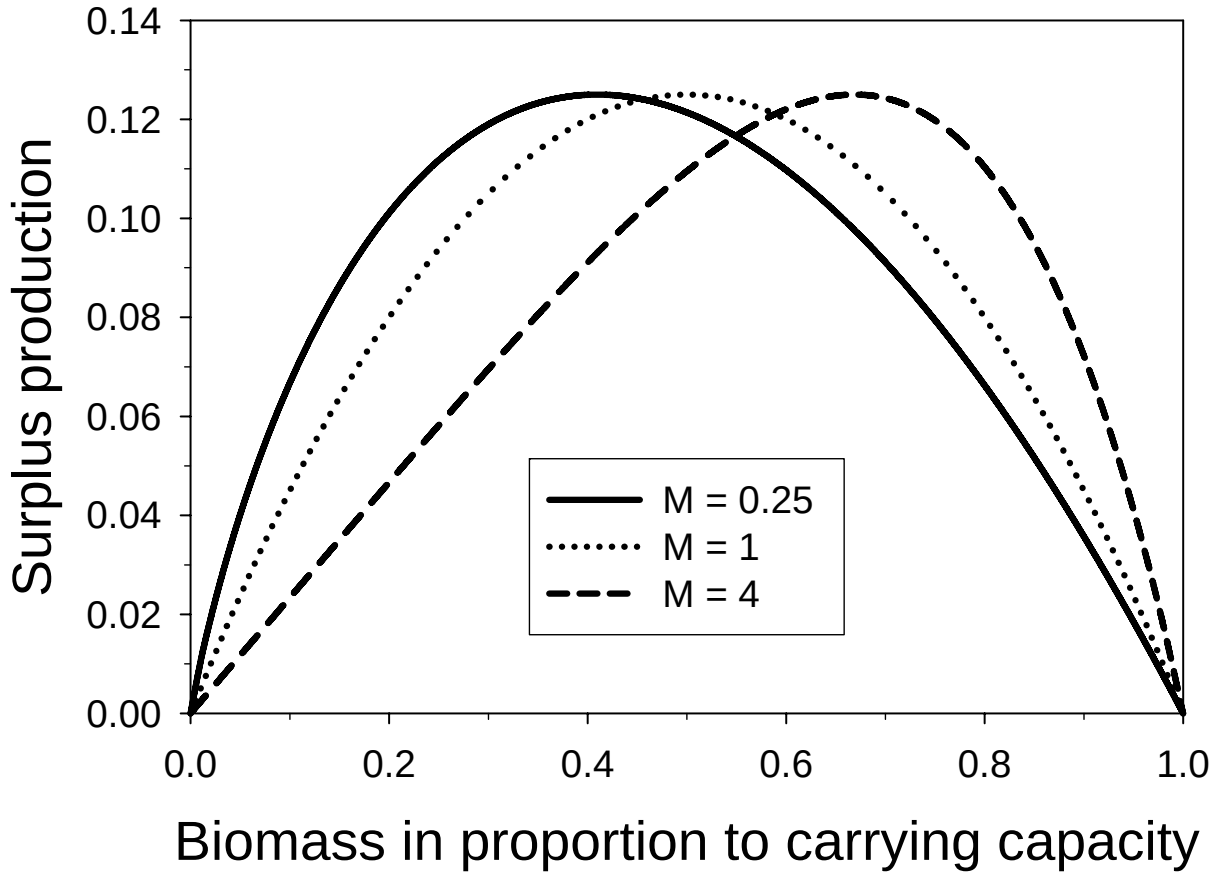

Figure 5.--Effect of shape parameter *M* on the relationship between surplus production and the biomass as a proportion of carrying capacity.

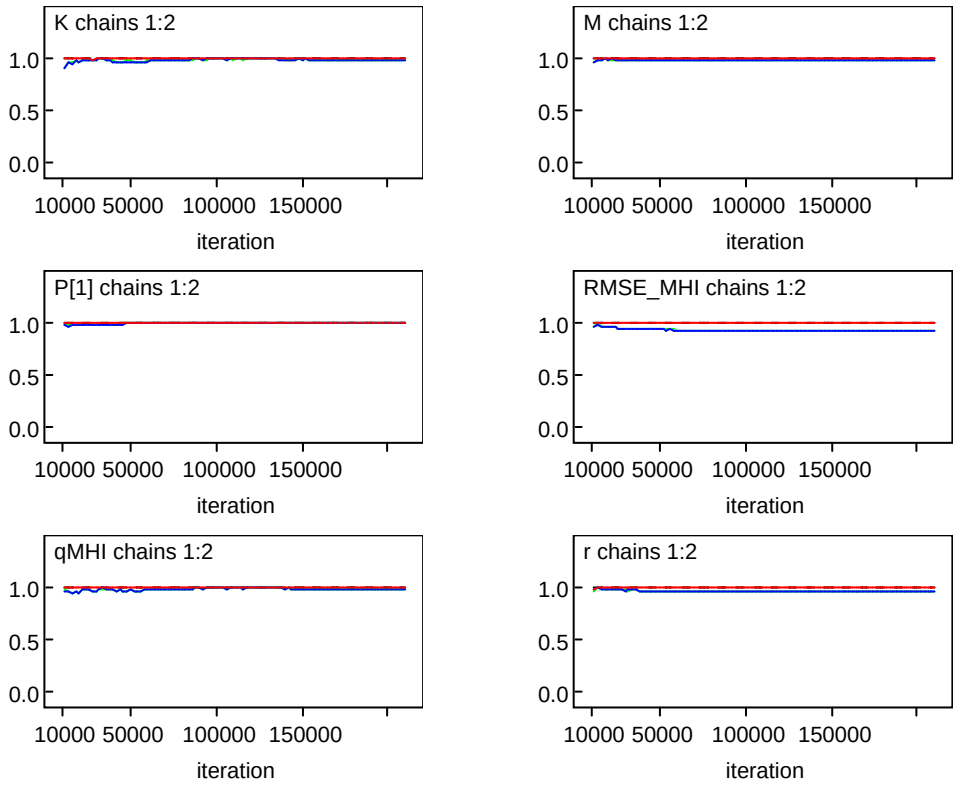

Figure 6.--Convergence diagnostic plots for carrying capacity (*K*), production shape parameter (*M*), initial proportion of carrying capacity (P[1], root-mean squared error (RMSE_MHI), catchability (*q*MHI), and intrinsic growth rate (*r*) estimates for MHI from the best fitting single-zone model.

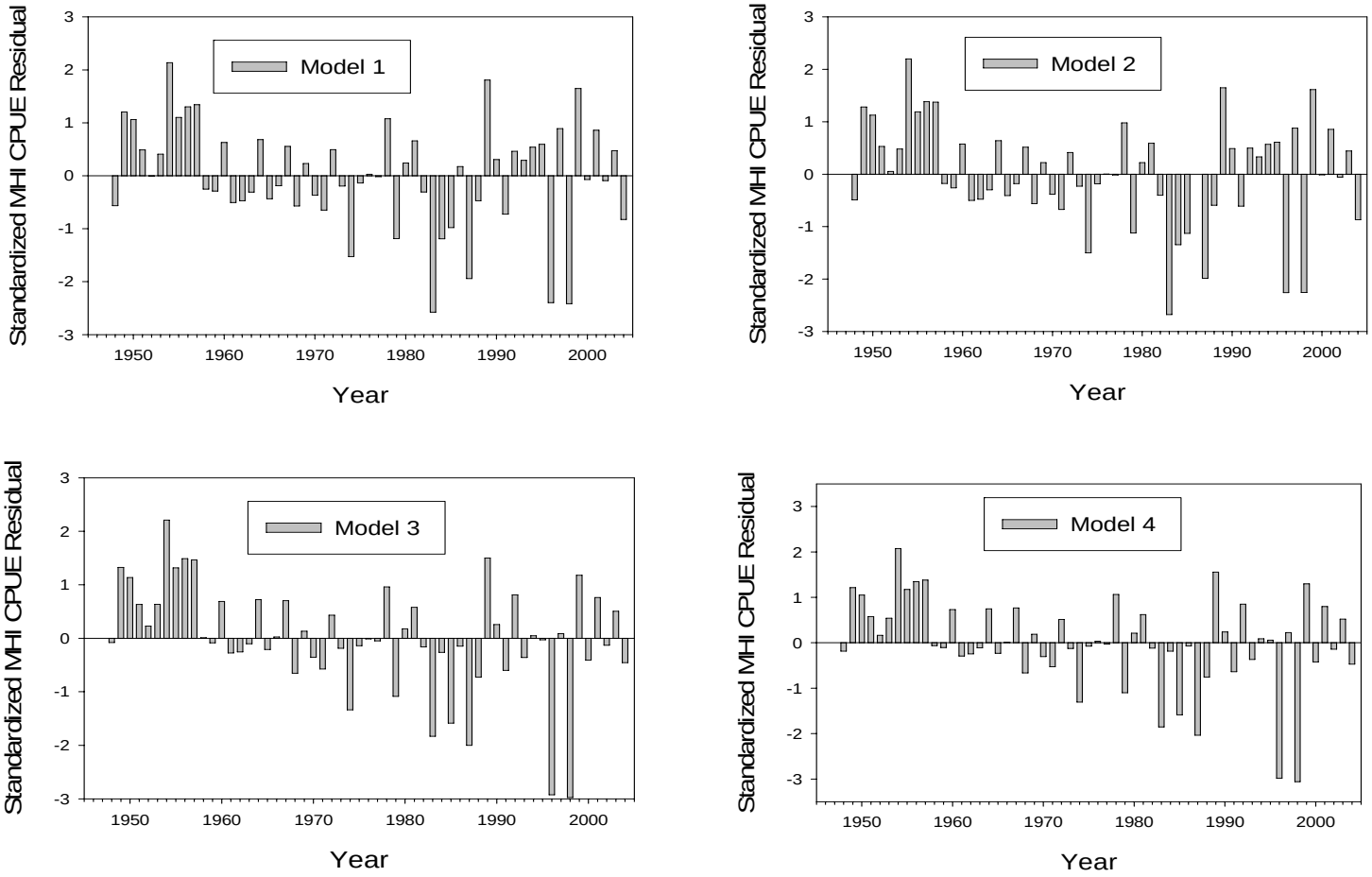

Figure 7.--Time series of standardized mean residuals for the single zone main Hawaiian Islands (MHI) bottomfish surplus production models, 1948–2004.

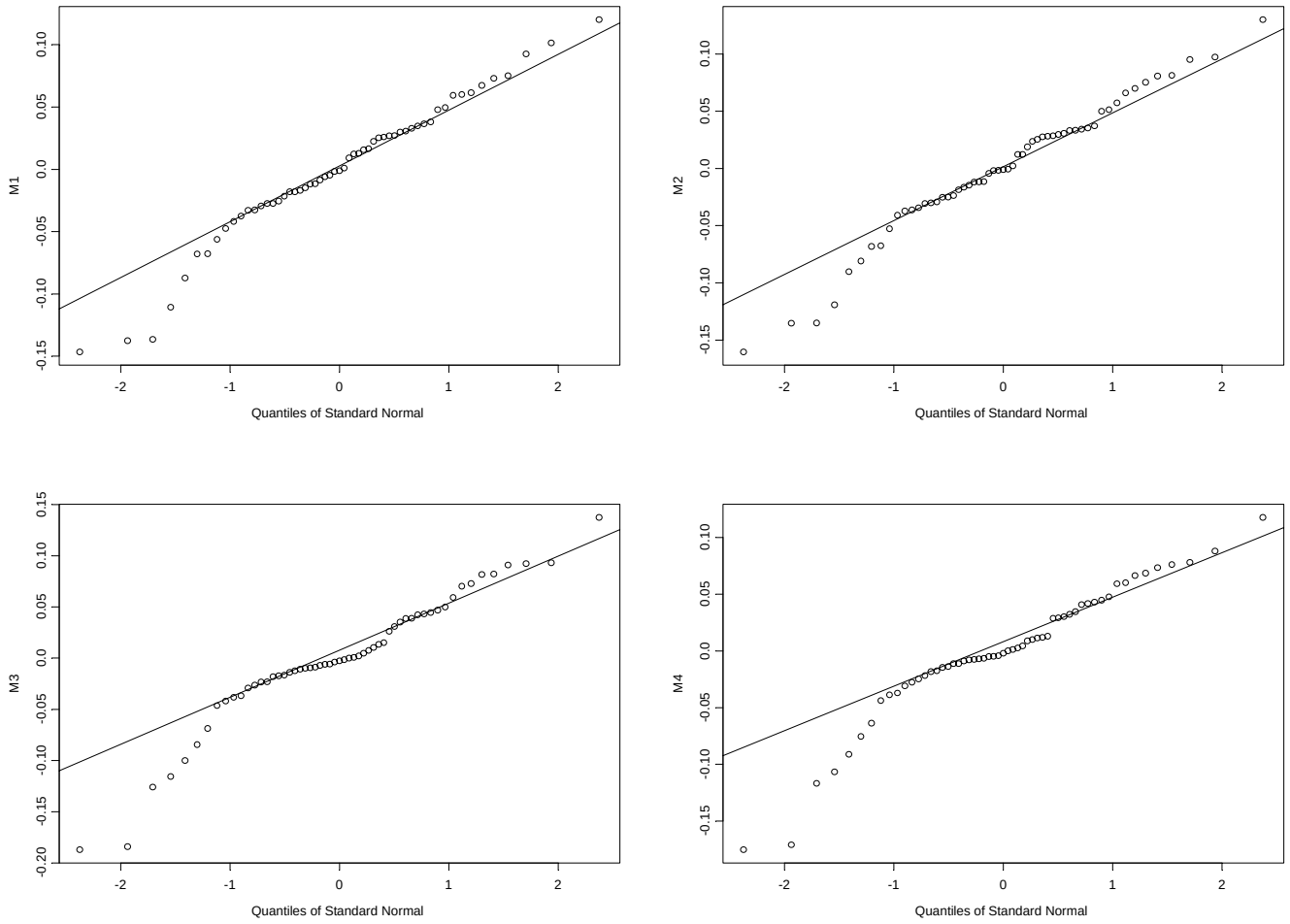

Figure 8.--Quantile-quantile plots of mean residuals of the single zone main Hawaiian Islands (MHI) bottomfish surplus production models during 1948-2004: model 1 (M1), model 2 (M2), model 3 (M3), and model 4 (M4).

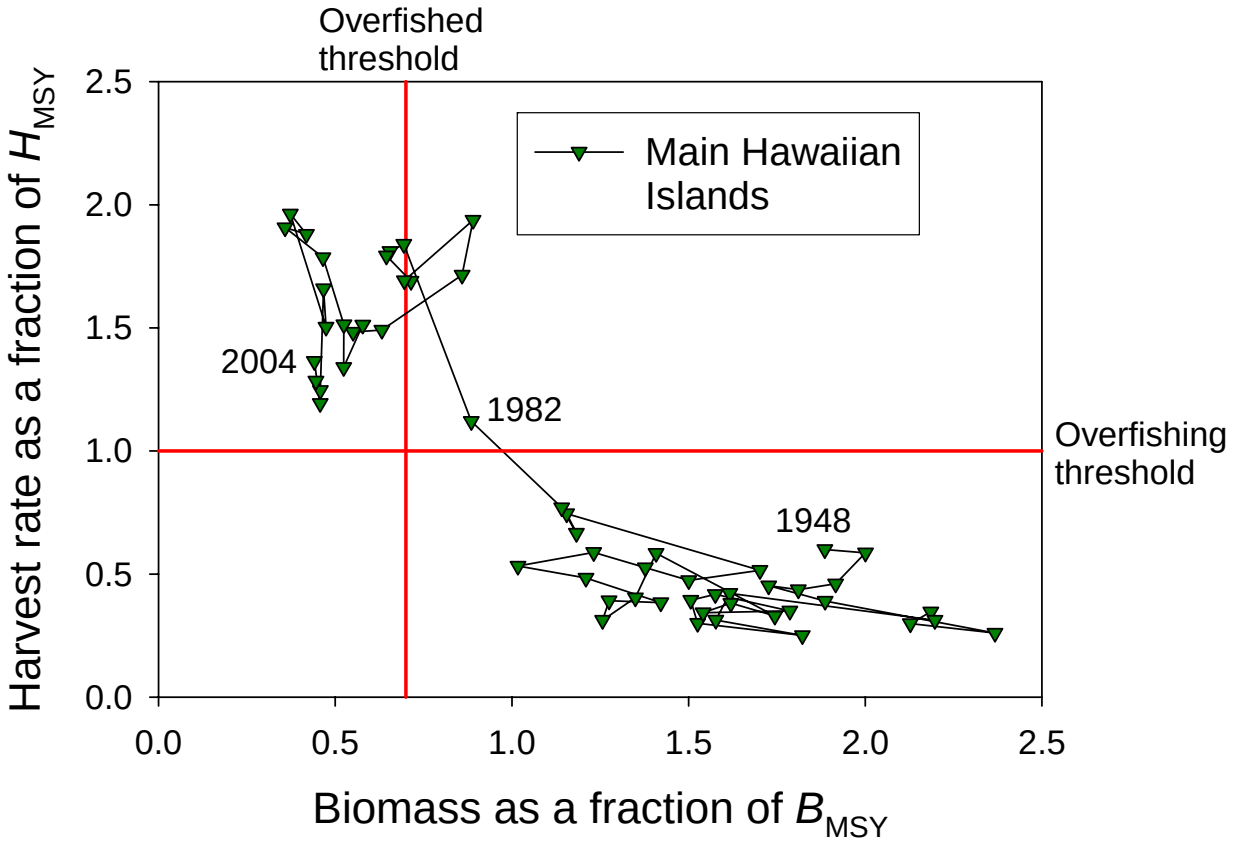

Figure 9.--Model averaged estimates of the hypothetical status of MHI bottomfish complex during 1948–2004 based on the single-zone MHI models if assessed as a separate management unit.

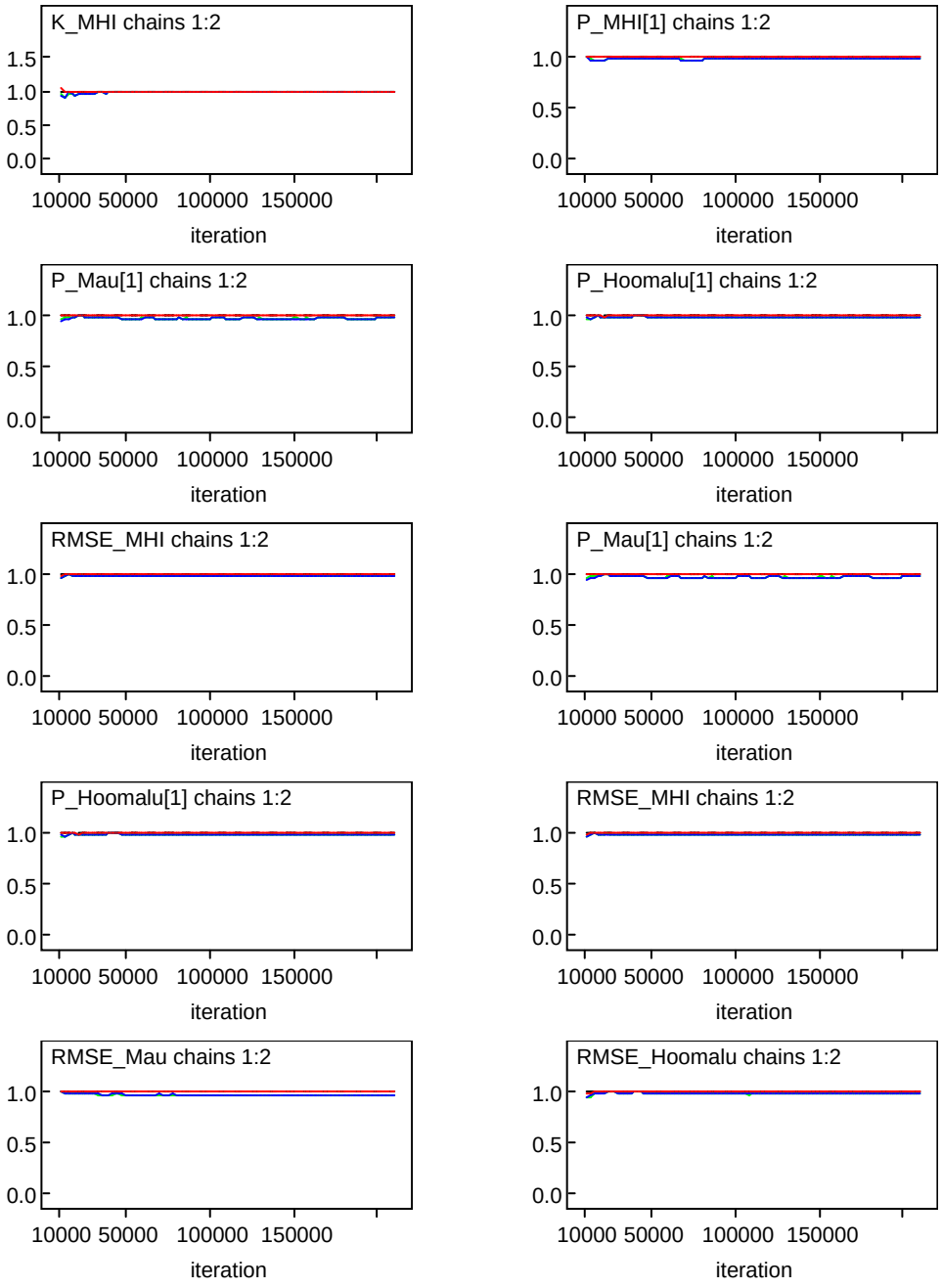

Figure 10.--Convergence diagnostic plots for MHI carrying capacity (K_MHI), initial proportions of carrying capacity by zone (P_*[1]), root-mean squared error by zone (RMSE_*), catchability by zone (q_*), and intrinsic growth rate (r) estimates from model 6, the most probable multizone model (p>0.99).

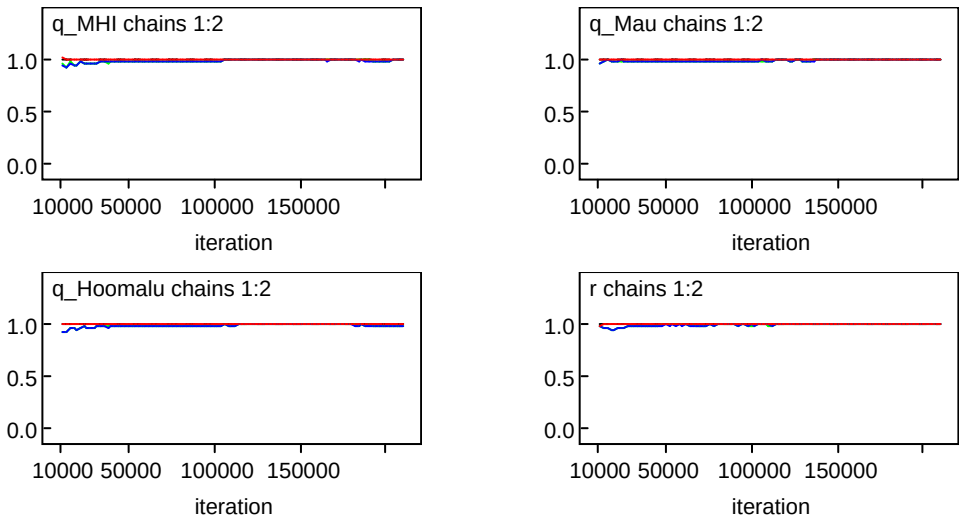

Figure 10.--Continued.

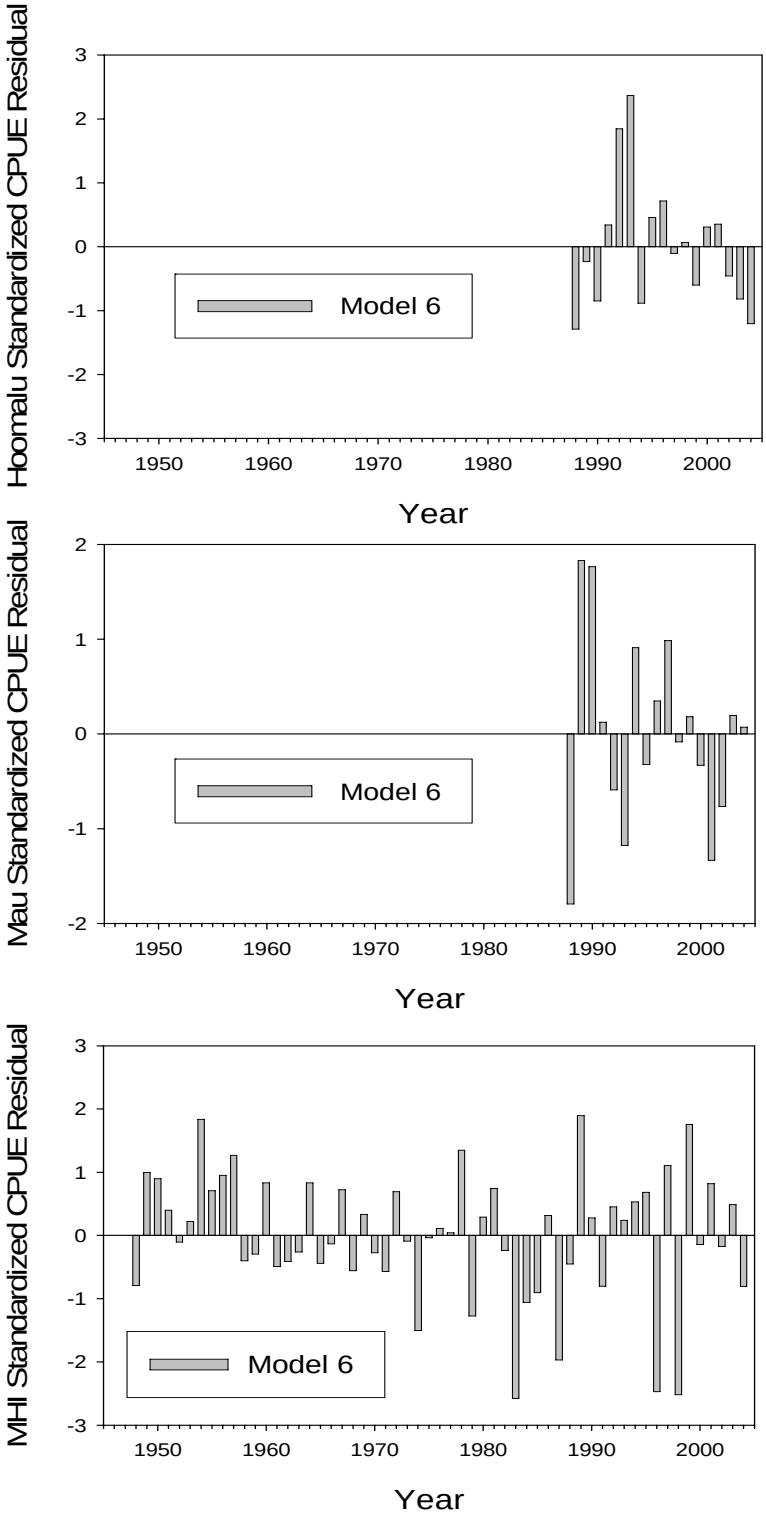

Figure 11.--Time series of standardized mean residuals for the most probable ($p > 0.99$) multizone bottomfish surplus production model fits to the Ho'omalu Zone, Mau Zone and main Hawaiian Islands (MHI) during 1948–2004.

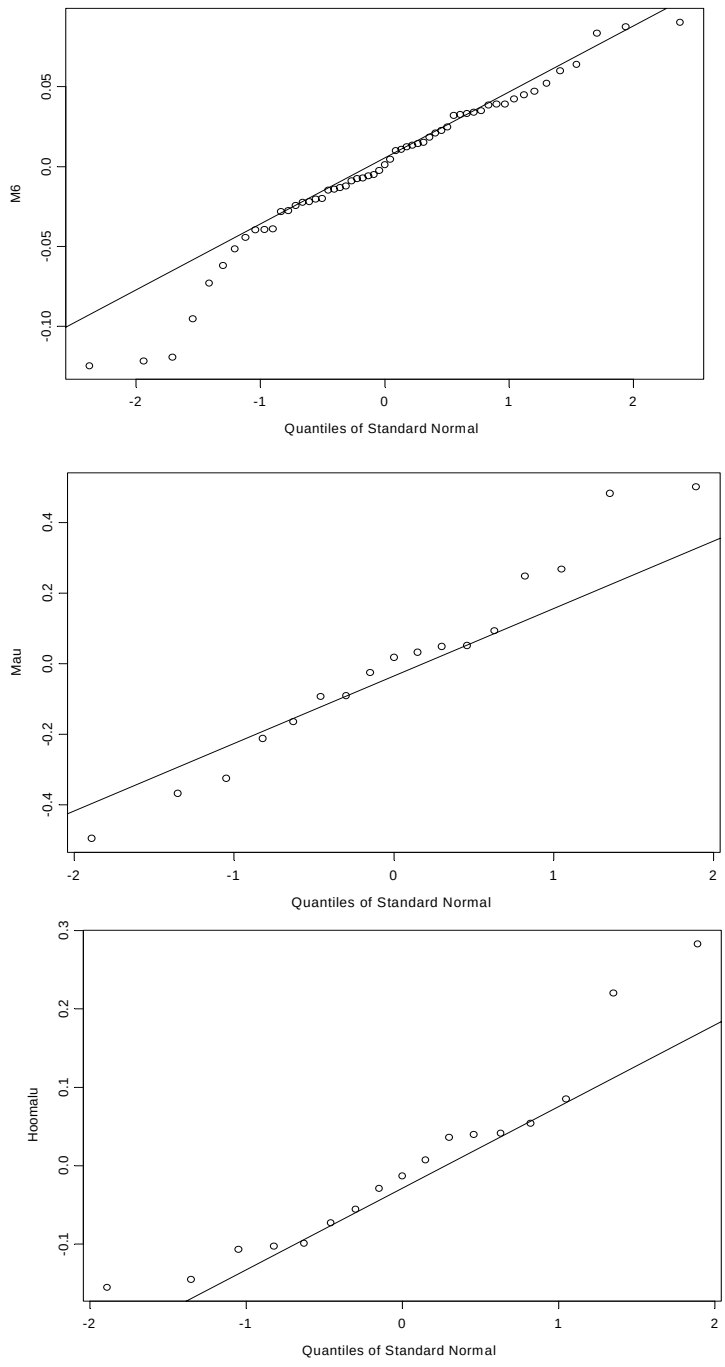

Figure 12.--Quantile-quantile plots of mean residuals of the most probable ($p >$ 0.99 multizone bottomfish surplus production model: main Hawaiian Islands (M6), Mau Zone (Mau), and Ho'omalu Zone (Ho'omalu).

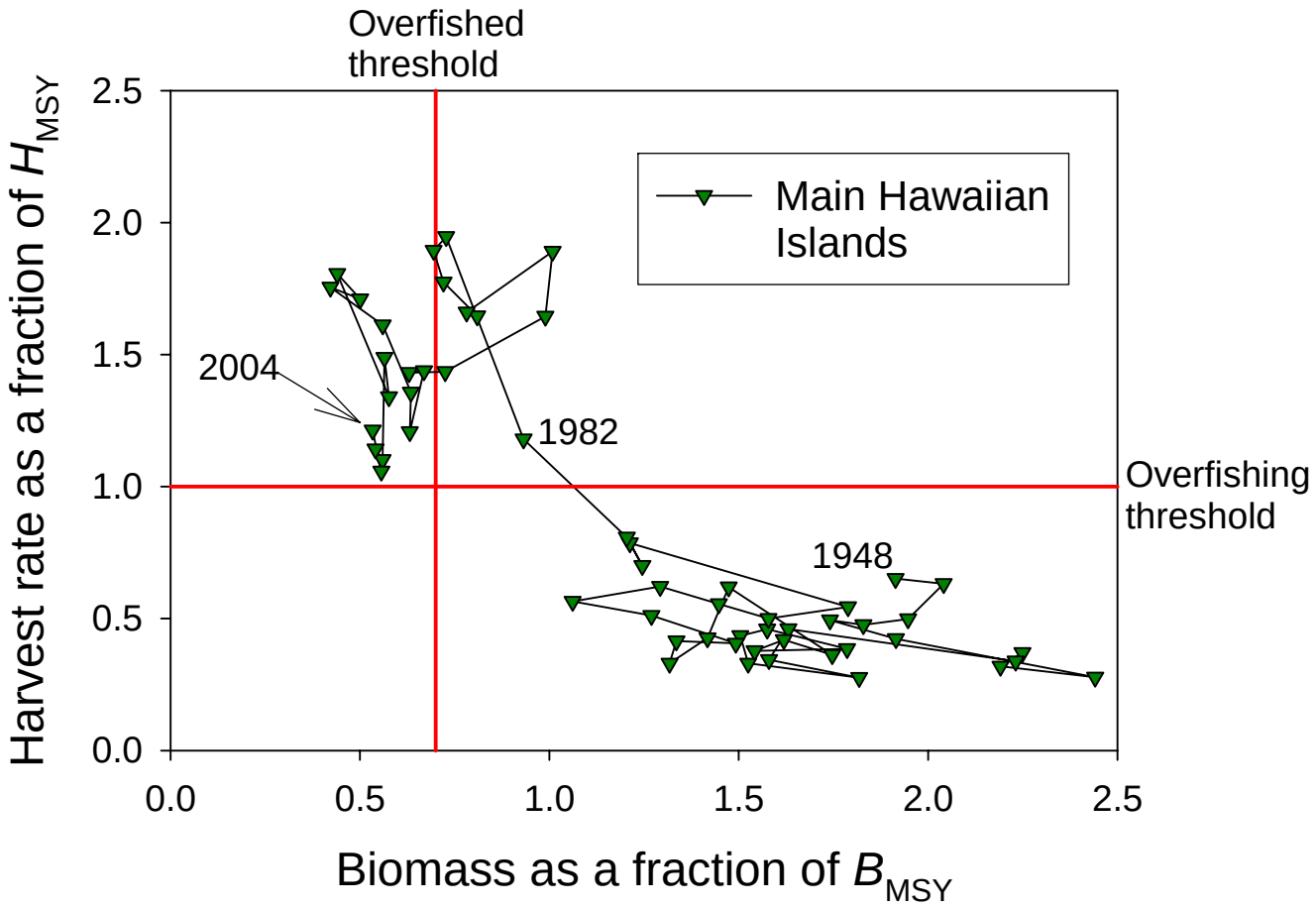

Figure 13.--Model averaged estimates of the hypothetical status of MHI bottomfish complex during 1948–2004 based on the MHI multizone models if assessed as a separate management unit..

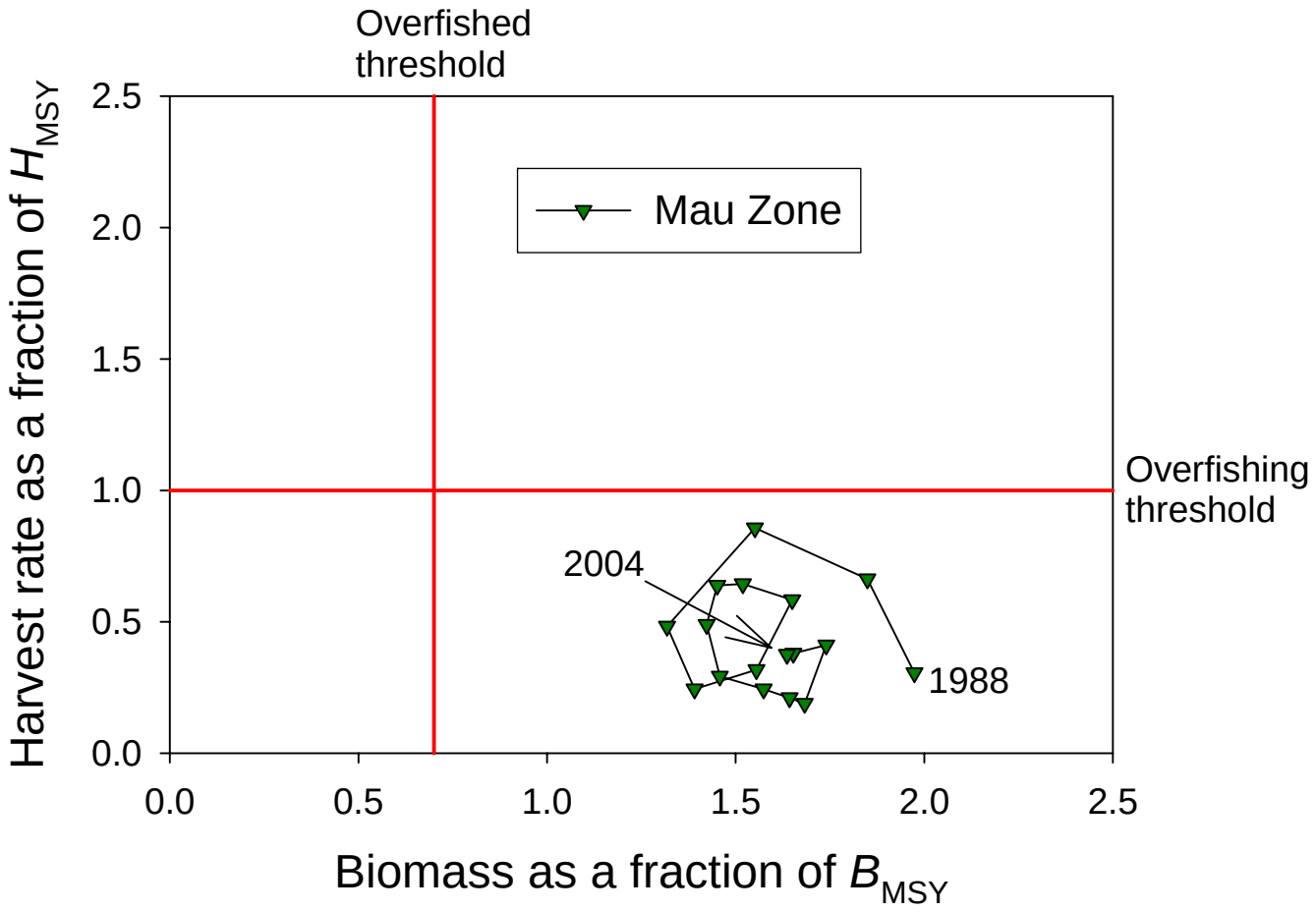

Figure 14.--Model averaged estimates of the hypothetical status of the Mau Zone bottomfish complex during 1948–2004 based on the Mau multizone models if assessed as a separate management unit..

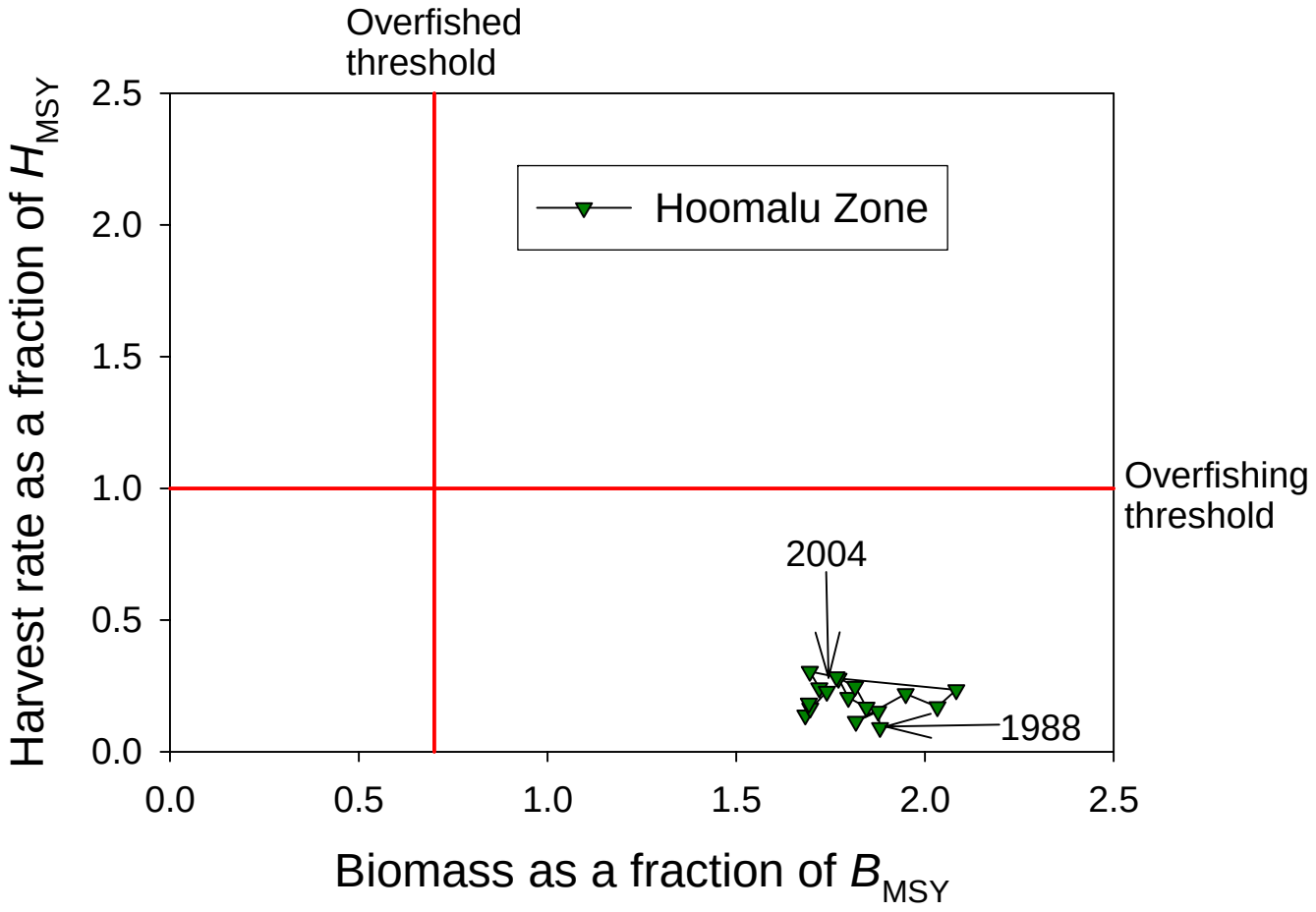

Figure 15.--Model averaged estimates of the hypothetical status of the Ho'omalu Zone bottomfish complex during 1948–2004 based on the Ho'omalu multizone models if assessed as a separate management unit.

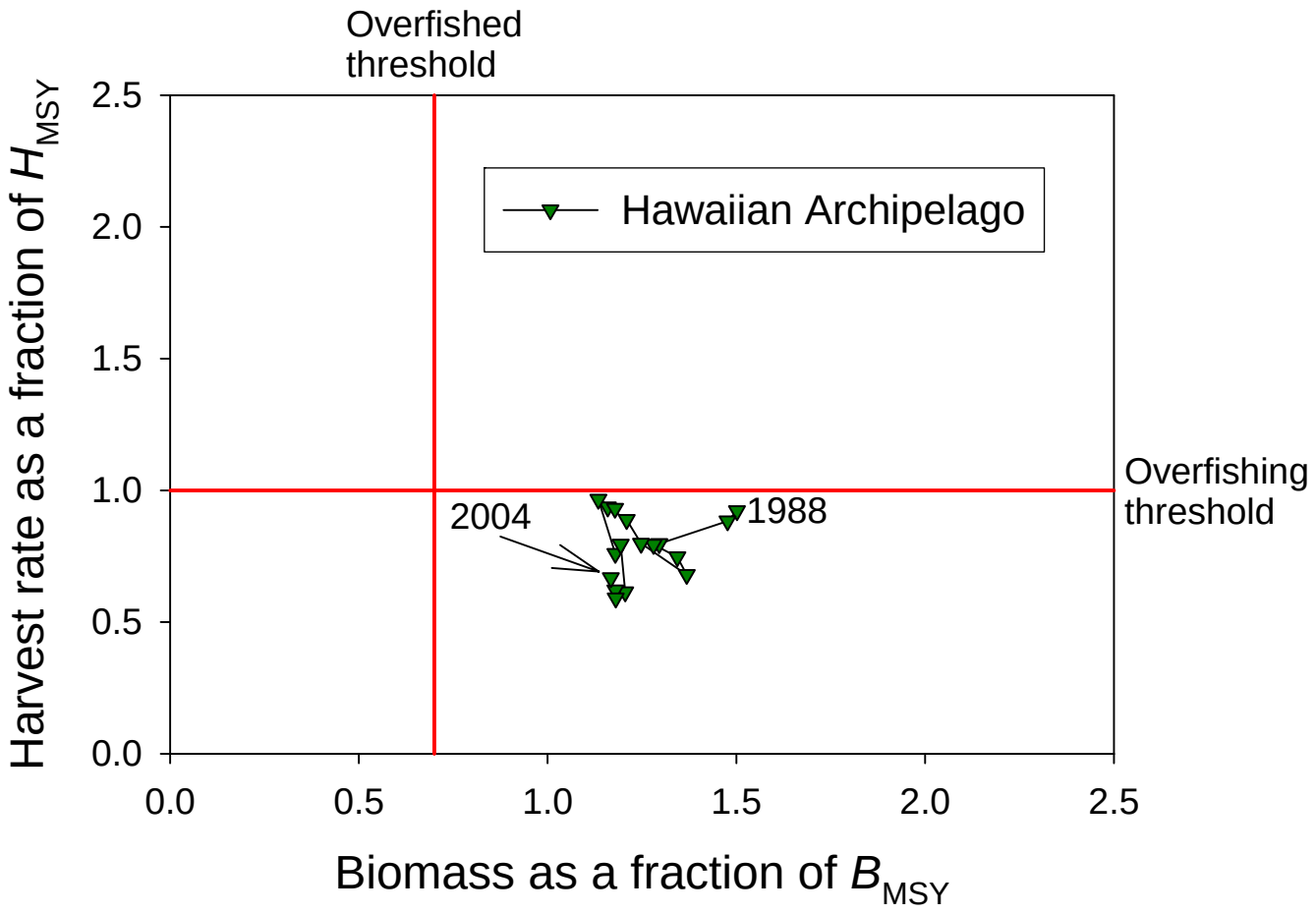

Figure 16.--Model averaged estimates of the hypothetical status of the Hawaiian Archipelago bottomfish complex during 1948–2004 based on the Hawaiian Archipelago multizone models if assessed using the alternative production modeling approach.

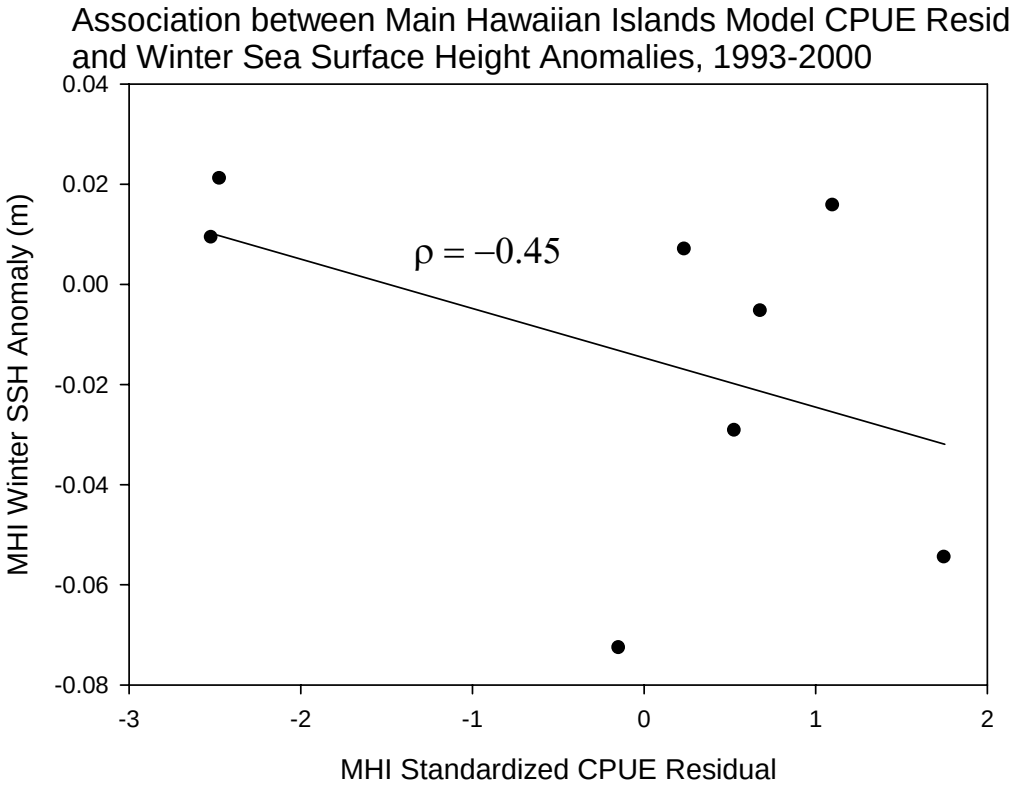

Figure 17.--Association (Pearson correlation coefficient ρ) between winter (January–March) SSH anomalies in the MHI during 1993–2000 and the MHI standardized CPUE residuals from the most probable ($p > 0.99$) multizone bottomfish surplus production model.

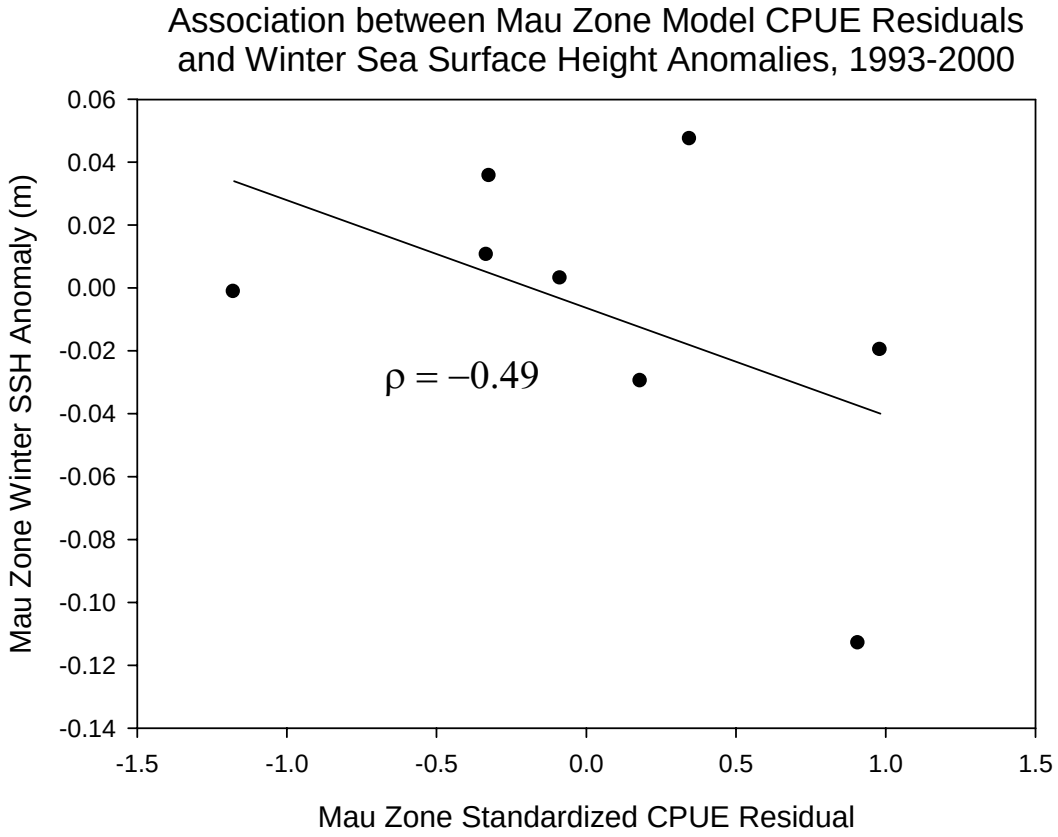

Figure 18.--Association (Pearson correlation coefficient ρ) between winter (January–March) SSH anomalies in the Mau Zone during 1993–2000 and the Mau Zone standardized CPUE residuals from the most probable ($p > 0.99$) multizone bottomfish surplus production model.

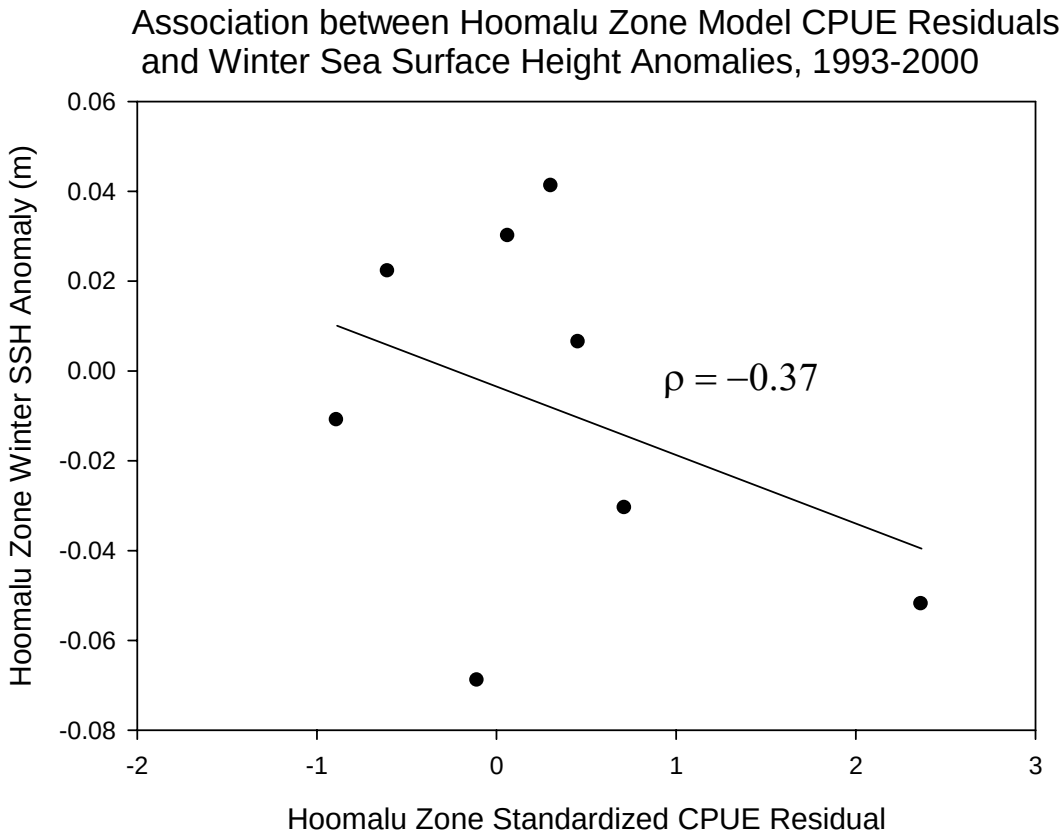

Figure 19.--Association (Pearson correlation coefficient ρ) between winter (January–March) SSH anomalies in the Ho'omalu Zone during 1993–2000 and the Ho'omalu Zone standardized CPUE residuals from the most probable ($p > 0.99$) multizone bottomfish surplus production model.

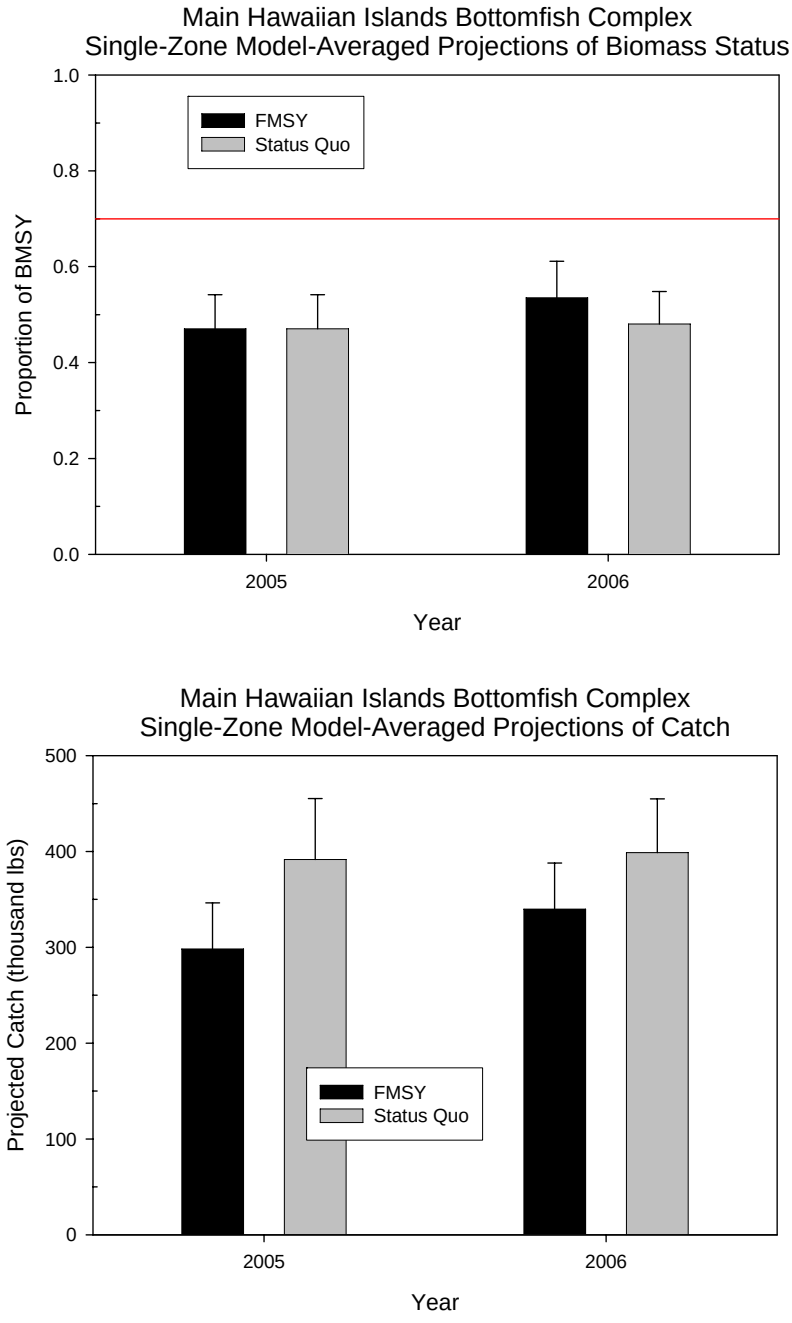

Figure 20.--Single-zone projections of biomass status and catch for MHI under two harvesting scenarios. Horizontal (red) line in upper graph is threshold for overfished status.

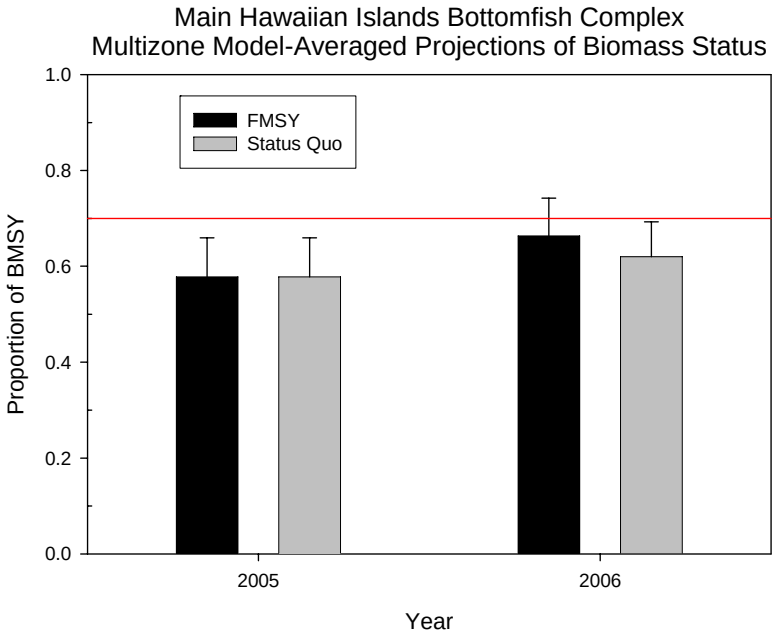

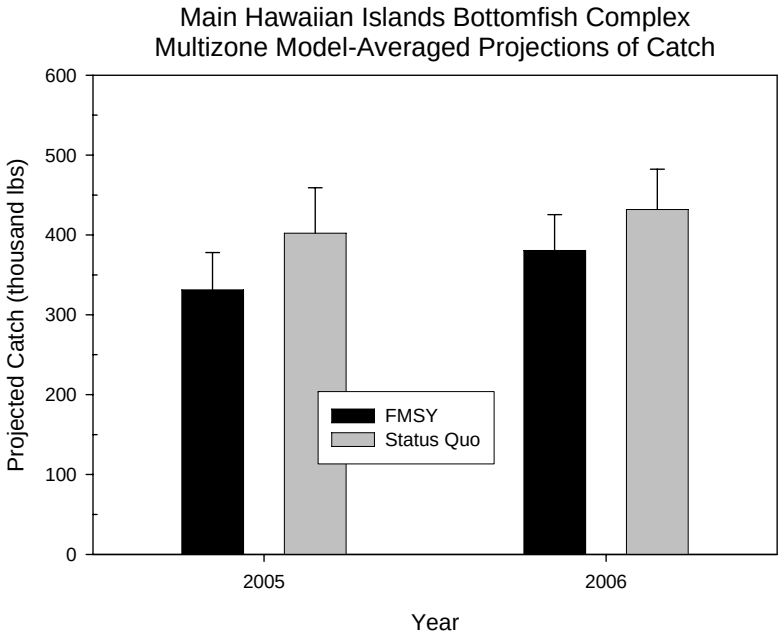

Figure 21.--Multizone projections of biomass status and catch for MHI under two harvesting scenarios. Horizontal (red) line in upper graph is threshold for overfished status.

Appendix. WINBUGS code to fit model 6, the most probable multizone bottomfish surplus production model, to MHI, Mau, and Ho'omalu Zone data.

Hawaiian Bottomfish: Archipelagic Assessment Bayesian State-Space Implementation of Schaefer Production Model

```
# Jon Brodziak, PIFSC, May 2006
# Catch units are thousands of pounds
# CPUE units are thousands of pounds per trip
# BFISH6 analyzes MHI catch & cpue data for 1948-2004
# BFISH6 analyzes Mau and Ho'omalu catch & cpue data for 1988-2004
# BFISH6 assumes no catch error
# BFISH6 assumes no changes in MHI catchability
# BFISH6 assumes a common intrinsic growth rate across regions, r
# BFISH6 estimates carrying capacity for MHI only
# BFISH6 assumes carrying capacities for Mau and Ho'omalu are proportional to habitat
#############################################################################

model BFISH6
{

# Prior distributions
#####################################################

# Diffuse normal prior for carrying capacity parameter, K
#(1)###################################################
K_MHI ~ dnorm(2000,0.00001)
K_Mau <- 0.277*K_MHI
K_Hoomalu <- 0.960*K_MHI

# Beta prior for intrinsic growth rate parameter, r
# with mean=0.5 and CV=20%
#(2)###################################################
 y ~ dbeta(12.0,12.0)
r <- 0.1+(0.9*y)

# Gamma priors for CPUE catchability coefficients
# within interval (0.0001,10), q
#(3)###################################################
iq_MHI ~ dgamma(0.001,0.001)I(0.1,10000)
q_MHI <- 1/iq_MHI
iq_Mau ~ dgamma(0.001,0.001)I(0.1,10000)
q_Mau <- 1/iq_Mau
iq_Hoomalu ~ dgamma(0.001,0.001)I(0.1,10000)
q_Hoomalu <- 1/iq_Hoomalu

# Gamma prior for process error variances, sigma2
#(4)###################################################
isigma2_MHI ~ dgamma(a0_MHI,b0_MHI)
sigma2_MHI <- 1/isigma2_MHI
isigma2_Mau ~ dgamma(a0_Mau,b0_Mau)
sigma2_Mau <- 1/isigma2_Mau
isigma2_Hoomalu ~ dgamma(a0_Hoomalu,b0_Hoomalu)
sigma2_Hoomalu <- 1/isigma2_Hoomalu

# Gamma priors for observation error variances, tau2
#(5)###################################################
itau2_MHI   ~ dgamma(c0_MHI,d0_MHI)
tau2_MHI   <- 1/itau2_MHI
itau2_Mau   ~ dgamma(c0_Mau,d0_Mau)
tau2_Mau   <- 1/itau2_Mau
itau2_Hoomalu   ~ dgamma(c0_Hoomalu,d0_Hoomalu)
tau2_Hoomalu   <- 1/itau2_Hoomalu
```

```
# Lognormal priors for time series of proportions of K, P
#(6)#####################################################
# MHI time series starts in 1948 and ends in 2004
Pmean_MHI[1] <- 0
P_MHI[1] ~ dlnorm(Pmean_MHI[1],isigma2_MHI) I(0.001,10)

# Process dynamics
for (i in 2:N_MHI) {
   Pmean_MHI[i] <- log(max(P_MHI[i-1] + r*P_MHI[i-1]*(1-P_MHI[i-1]) - Catch_MHI[i-1]/K_MHI,0.001))
    P_MHI[i]  ~ dlnorm(Pmean_MHI[i],isigma2_MHI)I(0.001,10)
   }

# Mau time series starts in 1988 and ends in 2004
Pmean_Mau[1] <- 0
P_Mau[1] ~ dlnorm(Pmean_Mau[1],isigma2_Mau) I(0.001,10)

# Process dynamics
for (i in 2:N_Mau) {
   Pmean_Mau[i] <- log(max(P_Mau[i-1] + r*P_Mau[i-1]*(1-P_Mau[i-1]) - Catch_Mau[i-1]/K_Mau,0.001))
    P_Mau[i]  ~ dlnorm(Pmean_Mau[i],isigma2_Mau)I(0.001,10)
   }

# Ho'omalu time series starts in 1988 and ends in 2004
Pmean_Hoomalu[1] <- 0
P_Hoomalu[1] ~ dlnorm(Pmean_Hoomalu[1],isigma2_Hoomalu) I(0.001,10)

# Process dynamics
for (i in 2:N_Hoomalu) {
   Pmean_Hoomalu[i] <- log(max(P_Hoomalu[i-1] + r*P_Hoomalu[i-1]*(1-P_Hoomalu[i-1]) - Catch_Hoomalu[i-1]/K_Hoomalu,0.001))
    P_Hoomalu[i]  ~ dlnorm(Pmean_Hoomalu[i],isigma2_Hoomalu)I(0.001,10)
   }

# Lognormal likelihood for observed CPUE indices
#(7)#####################################################
# MHI CPUE LIKELIHOOD 1948-2004 P_MHI[1:57], qMultiplier=1
for (i in 1:N_MHI) {
    CPUEmean_MHI[i] <- log(q_MHI*K_MHI*P_MHI[i])
    CPUE_MHI[i] ~ dlnorm(CPUEmean_MHI[i],itau2_MHI)
    RESID_MHI[i] <- log(CPUE_MHI[i]) - log(q_MHI*K_MHI*P_MHI[i])
          }
# Compute RMSE for MHI CPUE
RSS_MHI <- inprod(RESID_MHI[], RESID_MHI[])
RMSE_MHI <- sqrt(RSS_MHI/N_MHI)
AIC_MHI <- N_MHI*log(RSS_MHI/N_MHI)+2*NPAR_MHI
AICC_MHI <- AIC_MHI+2*NPAR_MHI*(NPAR_MHI+1)/(N_MHI-NPAR_MHI-1)

# Mau CPUE LIKELIHOOD 1988-2004 P_Mau[1:17], qMultiplier=1
for (i in 1:N_Mau) {
    CPUEmean_Mau[i] <- log(q_Mau*K_Mau*P_Mau[i])
    CPUE_Mau[i] ~ dlnorm(CPUEmean_Mau[i],itau2_Mau)
    RESID_Mau[i] <- log(CPUE_Mau[i]) - log(q_Mau*K_Mau*P_Mau[i])
          }
# Compute RMSE for Mau CPUE
RSS_Mau <- inprod(RESID_Mau[], RESID_Mau[])
RMSE_Mau <- sqrt(RSS_Mau/N_Mau)

# Ho'omalu CPUE LIKELIHOOD 1988-2004 P_Hoomalu[1:17], qMultiplier=1
for (i in 1:N_Hoomalu) {
    CPUEmean_Hoomalu[i] <- log(q_Hoomalu*K_Hoomalu*P_Hoomalu[i])
    CPUE_Hoomalu[i] ~ dlnorm(CPUEmean_Hoomalu[i],itau2_Hoomalu)
    RESID_Hoomalu[i] <- log(CPUE_Hoomalu[i]) - log(q_Hoomalu*K_Hoomalu*P_Hoomalu[i])
          }
# Compute RMSE for Ho'omalu CPUE
RSS_Hoomalu <- inprod(RESID_Hoomalu[], RESID_Hoomalu[])
RMSE_Hoomalu <- sqrt(RSS_Hoomalu/N_Hoomalu)

# Use total likelihood for overall AIC calculation
N_TOT <- N_MHI+N_Mau+N_Hoomalu
AIC_TOT<-
N_MHI*log(RSS_MHI/N_MHI)+N_Mau*log(RSS_Mau/N_Mau)+N_Hoomalu*log(RSS_Hoomalu/N_Hoomalu)+2*NPAR_TOT
```

```
AICC_TOT <- AIC_TOT+2*NPAR_TOT*(NPAR_TOT+1)/(N_TOT-NPAR_TOT-1)

# Compute exploitation rate and biomass time series
#(8)#####################################################
# MHI 1948-2004 P_MHI[1:57]
for (i in 1:N_MHI) {
    B_MHI[i] <- P_MHI[i]*K_MHI
    H_MHI[i] <- Catch_MHI[i]/B_MHI[i]
   }
P2005_MHI <- max(P_MHI[N_MHI]+r*P_MHI[N_MHI]*(1-P_MHI[N_MHI])-Catch_MHI[N_MHI]/K_MHI,0.001)
B2005_MHI <- P2005_MHI*K_MHI

# Mau 1988-2004 P_Mau[1:17]
for (i in 1:N_Mau) {
    B_Mau[i] <- P_Mau[i]*K_Mau
    H_Mau[i] <- Catch_Mau[i]/B_Mau[i]
   }
P2005_Mau <- max(P_Mau[N_Mau]+r*P_Mau[N_Mau]*(1-P_Mau[N_Mau])-Catch_Mau[N_Mau]/K_Mau,0.001)
B2005_Mau <- P2005_Mau*K_Mau

# Ho'omalu 1988-2004 P_Hoomalu[1:17]
for (i in 1:N_Hoomalu) {
    B_Hoomalu[i] <- P_Hoomalu[i]*K_Hoomalu
    H_Hoomalu[i] <- Catch_Hoomalu[i]/B_Hoomalu[i]
   }
P2005_Hoomalu <- max(P_Hoomalu[N_Hoomalu]+r*P_Hoomalu[N_Hoomalu]*(1-P_Hoomalu[N_Hoomalu])-
Catch_Hoomalu[N_Hoomalu]/K_Hoomalu,0.001)
B2005_Hoomalu <- P2005_Hoomalu*K_Hoomalu

# Compute reference points
#(9)#####################################################
# MHI Reference points
BMSP_MHI <- K_MHI/2
PMSP_MHI <- BMSP_MHI/K_MHI
MSP_MHI <- r*K_MHI/4
HMSP_MHI <- r/2
INDEXMSP_MHI <- q_MHI*BMSP_MHI
# MHI 1948-2004 BSTATUS_MHI and HSTATUS_MHI
for (i in 1:N_MHI) {
    BSTATUS_MHI[i] <- B_MHI[i]/BMSP_MHI
    HSTATUS_MHI[i] <- H_MHI[i]/HMSP_MHI
   }
# Count=1 if status ratio >= 1
p_MHI_above_BMSY <- step(BSTATUS_MHI[N_MHI] - 1.0)
p_MHI_above_HMSY <- step(HSTATUS_MHI[N_MHI] - 1.0)

# Mau Reference points
BMSP_Mau <- K_Mau/2
PMSP_Mau <- BMSP_Mau/K_Mau
MSP_Mau <- r*K_Mau/4
HMSP_Mau <- r/2
INDEXMSP_Mau <- q_Mau*BMSP_Mau
# Mau 1988-2004 BSTATUS_Mau and HSTATUS_Mau
for (i in 1:N_Mau) {
    BSTATUS_Mau[i] <- B_Mau[i]/BMSP_Mau
    HSTATUS_Mau[i] <- H_Mau[i]/HMSP_Mau
   }
# Count=1 if status ratio >= 1
p_Mau_above_BMSY <- step(BSTATUS_Mau[N_Mau] - 1.0)
p_Mau_above_HMSY <- step(HSTATUS_Mau[N_Mau] - 1.0)

# Ho'omalu Reference points
BMSP_Hoomalu <- K_Hoomalu/2
PMSP_Hoomalu <- BMSP_Hoomalu/K_Hoomalu
MSP_Hoomalu <- r*K_Hoomalu/4
HMSP_Hoomalu <- r/2
INDEXMSP_Hoomalu <- q_Hoomalu*BMSP_Hoomalu
# Ho'omalu 1988-2004 BSTATUS_Ho'omalu and HSTATUS_Ho'omalu
for (i in 1:N_Hoomalu) {
    BSTATUS_Hoomalu[i] <- B_Hoomalu[i]/BMSP_Hoomalu
```

```
    HSTATUS_Hoomalu[i] <- H_Hoomalu[i]/HMSP_Hoomalu
   }
# Count=1 if status ratio >= 1
p_Hoomalu_above_BMSY <- step(BSTATUS_Hoomalu[N_Hoomalu] - 1.0)
p_Hoomalu_above_HMSY <- step(HSTATUS_Hoomalu[N_Hoomalu] - 1.0)

# Archipelago Reference points
BMSP_Archipelago <- BMSP_MHI + BMSP_Mau + BMSP_Hoomalu
MSP_Archipelago <- MSP_MHI + MSP_Mau + MSP_Hoomalu
HMSP_Archipelago <- r/2
K_Archipelago <- K_MHI + K_Mau + K_Hoomalu
# Archipelago 1988-2004 BSTATUS_Archipelago and HSTATUS_Archipelago
for (i in 1:N_Mau) {
    BSTATUS_Archipelago[i] <-
weight_MHI*BSTATUS_MHI[i+40]+weight_Mau*BSTATUS_Mau[i]+weight_Hoomalu*BSTATUS_Hoomalu[i]
    HSTATUS_Archipelago[i] <-
weight_MHI*HSTATUS_MHI[i+40]+weight_Mau*HSTATUS_Mau[i]+weight_Hoomalu*HSTATUS_Hoomalu[i]
   }
# Count=1 if status ratio >= 1
p_Archipelago_above_BMSY <- step(BSTATUS_Archipelago[N_Mau] - 1.0)
p_Archipelago_above_HMSY <- step(HSTATUS_Archipelago[N_Mau] - 1.0)

# END OF CODE
###############################################################
}
```

Data

```
# Vector Catch() is total catch in thousand pounds
# Vector CPUE() is  the catch per unit effort index
# sigma2 is process error with parameters a0,b0
# tau2 is observation error with parameters c0,d0
#(10)#############################################################
list(
Catch_MHI=c(707.129,731.106,550.086,493.758,487.637,459.895,383.625,396.408,472.869,427.229,42
5.976,308.15,284.5,285.879,370.274,410.654,390.289,330.12,385.782,358.438,517.028,342.63,246.539,
314.096,343.249,368.054,339.85,455.507,455.871,447.279,550.464,540.68,494.952,551.978,623.68,801
.925,746.353,725.768,756.894,736.004,1083.039,922.349,590.45,511.406,546.445,432.877,488.591,512
.52,420.063,485.86,450.859,437.861,476.763,349.469,350.701,334.058,366.358),
CPUE_MHI=c(0.614,0.713,0.677,0.621,0.577,0.645,0.887,0.755,0.784,0.789,0.533,0.519,0.63,0.496,0.4
91,0.518,0.619,0.503,0.536,0.602,0.478,0.48,0.433,0.433,0.514,0.421,0.329,0.43,0.485,0.527,0.635,0.38
,0.421,0.416,0.307,0.214,0.22,0.23,0.274,0.237,0.329,0.361,0.245,0.202,0.228,0.213,0.217,0.193,0.125,
0.176,0.13,0.209,0.187,0.194,0.179,0.19,0.171),
N_MHI=57, NPAR_MHI=6, NPAR_TOT=14,
a0_MHI=4.0,b0_MHI=0.01,
c0_MHI=2.0,d0_MHI=0.01,
weight_MHI=0.447,
Catch_Mau=c(95.137,193.038,209.063,99.887,53.249,77.476,151.088,153.686,145.215,109.004,66.723,
60.264,54.276,49.927,112.376,98.728,96.547),
CPUE_Mau=c(2.136,5.412,4.454,2.413,2.092,1.992,3.748,2.46,2.823,3.294,2.518,2.926,2.654,2.066,2.4
96,3.086,2.953),
N_Mau=17,
a0_Mau=4.0,b0_Mau=0.01,
c0_Mau=2.0,d0_Mau=0.01,
weight_Mau=0.124,
Catch_Hoomalu=c(93.465,156.813,113.53,233.651,188.604,264.283,269.027,201.173,169.241,244.803,
273.844,281.984,226.935,217.447,127.33,151.748,169.238),
CPUE_Hoomalu=c(4.702,5.328,4.793,5.928,7.388,8.04,4.651,5.544,5.87,5.234,5.198,4.606,5.212,5.3,4.
651,4.483,4.272),
N_Hoomalu=17,
a0_Hoomalu=4.0,b0_Hoomalu=0.01,
c0_Hoomalu=2.0,d0_Hoomalu=0.01,
```

```
weight_Hoomalu=0.429
)
```

Inits

```
#(11)############################################################
# Initial Condition 1
list(
y=0.5,
P_MHI=c(0.9,0.9,0.9,0.9,0.9,0.9,0.9,0.9,0.9,0.9,0.9,0.9,0.9,0.9,0.9,0.9,0.9,0.9,0.9,0.9,0.9,0.9,0.9,0.9,0.9,0
.9,0.9,0.9,0.9,0.9,0.75,0.75,0.75,0.75,0.75,0.75,0.75,0.75,0.75,0.5,0.5,0.5,0.5,0.5,0.5,0.5,0.5,0.5,0.5,
0.5,0.5,0.5,0.5,0.5,0.5,0.5),
K_MHI=2000,
iq_MHI=1000,
isigma2_MHI=100,
itau2_MHI=100
P_Mau=c(0.5,0.5,0.5,0.5,0.5,0.5,0.5,0.5,0.5,0.5,0.5,0.5,0.5,0.5,0.5,0.5,0.5),
iq_Mau=1000,
isigma2_Mau=100,
itau2_Mau=100
P_Hoomalu=c(0.5,0.5,0.5,0.5,0.5,0.5,0.5,0.5,0.5,0.5,0.5,0.5,0.5,0.5,0.5,0.5,0.5),
iq_Hoomalu=1000,
isigma2_Hoomalu=100,
itau2_Hoomalu=100
)
# Initial Condition 2
list(
y=0.75,
P_MHI=c(0.9,0.9,0.9,0.9,0.9,0.9,0.9,0.9,0.9,0.9,0.9,0.9,0.9,0.9,0.9,0.9,0.9,0.9,0.9,0.9,0.9,0.9,0.9,0.9,0.9,0
.9,0.9,0.9,0.9,0.9,0.75,0.75,0.75,0.75,0.75,0.75,0.75,0.75,0.75,0.5,0.5,0.5,0.5,0.5,0.5,0.5,0.5,0.5,0.5,
0.5,0.5,0.5,0.5,0.5,0.5,0.5),
K_MHI=1000,
iq_MHI=1000,
isigma2_MHI=100,
itau2_MHI=100
P_Mau=c(0.5,0.5,0.5,0.5,0.5,0.5,0.5,0.5,0.5,0.5,0.5,0.5,0.5,0.5,0.5,0.5,0.5),
iq_Mau=1000,
isigma2_Mau=100,
itau2_Mau=100
P_Hoomalu=c(0.5,0.5,0.5,0.5,0.5,0.5,0.5,0.5,0.5,0.5,0.5,0.5,0.5,0.5,0.5,0.5,0.5),
iq_Hoomalu=1000,
isigma2_Hoomalu=100,
itau2_Hoomalu=100
)
```